

BRIGHAM YOUNG UNIVERSITY

GEOLOGY STUDIES

VOLUME 27, PART 1

AUGUST 1980



BRIGHAM YOUNG UNIVERSITY GEOLOGY STUDIES

Volume 27, Part 1

- Preble Formation, a Cambrian Outer Continental Shelf Deposit in Nevada M. N. Rees and A. J. Rowell
- The Fitchville Formation: A Study of the Biostratigraphy and Depositional Environments in
West Central Utah County, Utah Brian R. Greenhalgh
- Sandstone and Conglomerate-Breccia Pipes and Dikes of the Kodachrome Basin Area, Kane County, Utah Cheryl Hannum
- Exhumed Paleochannels in the Lower Cretaceous Cedar Mountain Formation near Green River, Utah Daniel R. Harris
- The Stratigraphy and Structure of the Cedar Hills, Sanpete County, Utah Ralph L. Hawks, Jr.
- Paleoenvironments of the Lower Triassic Thaynes Formation, near Diamond Fork in Spanish Fork Canyon,
Utah County, Utah Bruce H. James
- A Gravity Study of the Nampa-Caldwell Area, Canyon County, Idaho J. Roger Olsen
- Geology of the Sterling Quadrangle, Sanpete County, Utah James Michael Taylor

Publications and Maps of the Geology Department



Cover: Aerial photograph showing exhumed stream paleochannels in the Cedar Mountain Formation near Green River, Utah. Courtesy Daniel R. Harris.

A publication of the
Department of Geology
Brigham Young University
Provo, Utah 84602

Editors

W. Kenneth Hamblin
Cynthia M. Gardner

Brigham Young University Geology Studies is published by the department. *Geology Studies* consists of graduate-student and staff research in the department and occasional papers from other contributors. *Studies for Students* supplements the regular issues and is intended as a series of short papers of general interest which may serve as guides to the geology of Utah for beginning students and laymen.

ISSN 0068-1016

Distributed August 1980

8-80 600 43937

CONTENTS

<p>Preble Formation, a Cambrian Outer Continental Shelf Deposit in Nevada 1</p> <p>Abstract 1</p> <p>Introduction 1</p> <p>Preble Formation 1</p> <p style="padding-left: 20px;">Definition and age 1</p> <p style="padding-left: 20px;">Thickness and stratigraphic subdivision 2</p> <p>Interpretation of lithology and depositional setting 3</p> <p style="padding-left: 20px;">Lower Preble Formation 3</p> <p style="padding-left: 20px;">Middle Preble Formation 4</p> <p style="padding-left: 20px;">Upper Preble Formation 7</p> <p>Acknowledgments 8</p> <p>References cited 8</p> <p>Figures</p> <p style="padding-left: 20px;">1. Principal outcrops of Preble Formation and index of localities mentioned in text 1</p> <p style="padding-left: 20px;">2. Outcrop patterns of gravity-flow deposits and principal faults 2</p> <p style="padding-left: 20px;">3. Geological sketch map 3</p> <p style="padding-left: 20px;">4. Thrust recumbent folds 3</p> <p style="padding-left: 20px;">5. Negative print of bioclastic grainstone 4</p> <p style="padding-left: 20px;">6. Outcrop of alternating carbonate turbidity deposits and shale 5</p> <p style="padding-left: 20px;">7. Sediment gravity-flow deposit 5</p> <p style="padding-left: 20px;">8. Oolite with interbeds and lenses of dolomitic mudstone 6</p> <p style="padding-left: 20px;">9. Photomicrograph: Contact between oolite and overlying dolomitic mudstone 6</p> <p style="padding-left: 20px;">10. Upper Cambrian thin-bedded dolomitic limestone and shale 7</p> <p>The Fitchville Formation: A Study of the Biostratigraphy and Depositional Environments in West Central Utah County, Utah 9</p> <p>Introduction 9</p> <p style="padding-left: 20px;">Acknowledgments 9</p> <p style="padding-left: 20px;">Previous work 9</p> <p style="padding-left: 20px;">Procedures 10</p> <p>Paleogeography and paleotectonic setting 11</p> <p>Stratigraphy 12</p> <p style="padding-left: 20px;">Stratigraphic units 12</p> <p style="padding-left: 20px;">Dolomitization 14</p> <p>Paleoecology 14</p> <p style="padding-left: 20px;">The paleoecology of Fitchville corals 14</p> <p style="padding-left: 20px;">The paleoecology of Fitchville brachiopods 14</p> <p style="padding-left: 20px;">The paleoecology of conodonts 15</p> <p style="padding-left: 20px;">Orientations 15</p> <p style="padding-left: 20px;">Associations 15</p> <p style="padding-left: 20px;">Abundances 15</p> <p>Depositional environments 17</p> <p style="padding-left: 20px;">Introduction 17</p> <p style="padding-left: 20px;">Quartz clastic layers 17</p> <p style="padding-left: 20px;">The lower (Devonian) limestones (units 2a and 2b) 19</p> <p style="padding-left: 20px;">The lower (Devonian) dolomites (units 3-5) 19</p> <p style="padding-left: 20px;">The upper (Mississippian) dolomites (units 6 and 7) 20</p> <p style="padding-left: 20px;">The upper (Mississippian) limestones (units 8 and 9) 20</p> <p style="padding-left: 20px;">The curly limestone (unit 10) 20</p> <p style="padding-left: 20px;">The lowermost Gardison limestones (units 11-14) 23</p>	<p>Biostratigraphy 23</p> <p style="padding-left: 20px;">The lower (Famennian) limestones (units 2a and 2b) 23</p> <p style="padding-left: 20px;">The lower (Famennian) dolomites (units 3-5) 24</p> <p style="padding-left: 20px;">The upper (Kinderhookian) dolomites (units 6 and 7) 24</p> <p style="padding-left: 20px;">The upper (Kinderhookian) limestones (units 8-10) 25</p> <p style="padding-left: 20px;">The lowermost (Osagean) Gardison limestones (units 11-14) 25</p> <p>Conclusions 25</p> <p>Appendix A 25</p> <p>Appendix B 27</p> <p>References cited 29</p> <p>Figures</p> <p style="padding-left: 20px;">1. Index map of the study area 10</p> <p style="padding-left: 20px;">2. Wanlass Hill viewed from the south 10</p> <p style="padding-left: 20px;">3. Greeley Hill viewed from the southwest 11</p> <p style="padding-left: 20px;">4. Basal sand-grain layer (unit 1) 12</p> <p style="padding-left: 20px;">5. Stratigraphy, correlation, and zonation chart 13</p> <p style="padding-left: 20px;">6. Association of <i>Syringopora surcularia</i> and <i>S. hisingeri</i> 16</p> <p style="padding-left: 20px;">7. Carbonate sedimentation model of Irwin (1965) 17</p> <p style="padding-left: 20px;">8. Photomicrograph of basal sand-grain layer 17</p> <p style="padding-left: 20px;">9. Sand-filled burrows of unit 5 18</p> <p style="padding-left: 20px;">10. Distorted <i>Syringopora</i> and burrowed layer of unit 5 18</p> <p style="padding-left: 20px;">11. Photomicrograph of intraclasts in unit 9 20</p> <p style="padding-left: 20px;">12. Curly bed, with stromatolitic dome 21</p> <p style="padding-left: 20px;">13. Photomicrograph of the curly-bed laminations 22</p> <p style="padding-left: 20px;">14. Photomicrograph of the curly bed with <i>Sphaerocodium</i>? 22</p> <p>Tables</p> <p style="padding-left: 20px;">1. Abundances of <i>Syringopora</i> corals on Wanlass Hill 11</p> <p style="padding-left: 20px;">2. Abundances of solitary rugose corals on Wanlass Hill 11</p> <p>Sandstone and Conglomerate-Breccia Pipes and Dikes of the Kodachrome Basin Area, Kane County, Utah 31</p> <p>Abstract 31</p> <p>Introduction 31</p> <p style="padding-left: 20px;">Location 31</p> <p style="padding-left: 20px;">Previous work 31</p> <p style="padding-left: 20px;">Methods of study 32</p> <p style="padding-left: 20px;">Structure and regional setting 33</p> <p style="padding-left: 20px;">Acknowledgments 34</p> <p>Stratigraphy 34</p> <p style="padding-left: 20px;">Navajo Sandstone 34</p> <p style="padding-left: 20px;">Carmel Formation 34</p> <p style="padding-left: 40px;">Judd Hollow Tongue 34</p> <p style="padding-left: 40px;">Thousand Pockets Tongue of the Navajo Sandstone 34</p> <p style="padding-left: 20px;">Paria River Member 34</p> <p style="padding-left: 20px;">Winsor Member 34</p> <p style="padding-left: 20px;">Wiggler Wash Member 34</p> <p style="padding-left: 20px;">Entrada Sandstone 35</p> <p style="padding-left: 40px;">Gunsight Butte Member 35</p> <p style="padding-left: 40px;">Cannonville Member 35</p> <p style="padding-left: 40px;">Escalante Member 35</p> <p style="padding-left: 20px;">Pre-Morrison unconformity 36</p> <p style="padding-left: 20px;">Henrieville Sandstone 36</p> <p style="padding-left: 20px;">Sub-Cretaceous unconformity 36</p> <p style="padding-left: 20px;">Dakota Formation 36</p>
---	---

Distribution of pipes and dikes	36	30. Photomicrograph: Thin section of thin dike between pipes 10 and 11	47
Description of representative pipes and dikes	36	Exhumed Paleochannels in the Lower Cretaceous Cedar Mountain Formation near Green River, Utah	51
Pipe 3	36	Abstract	51
Pipe 27	36	Introduction	51
Pipe 28	37	Location	51
Pipe area 29	37	Previous work	51
Pipe 34	39	Methods	53
Pipe 35	39	Acknowledgments	53
Pipe 38	40	Geologic setting	53
Pipe 43	40	Stratigraphy	53
Dike 49	40	Morrison Formation	54
Pipe 51	41	Cedar Mountain Formation	54
Pipe 52	41	Dakota Formation	54
Mancos Formation	54	Channel classification	56
Composition	41	Channel dimensions	56
Country rock	41	Channel A	56
Sandstone and conglomerate pipes and dikes	43	Channel B	56
Channel C	56	Channel C	56
Channel D	57	Channel D	57
Generalized types of pipes and dikes in the Kodachrome Basin area	45	Channel patterns	57
Sandstone pipes	45	Sinuosity	58
Conglomerate-breccia pipes	45	Point-bar and channel-fill deposits	58
Thick extensive dikes	46	Point-bar deposits	58
Thin dikes	46	Channel fills	60
Conclusions	46	Sedimentary structures	60
Observations and comparisons	46	Primary structures	60
Interpretation	48	Secondary structures	61
References cited	49	Vertical sequence	62
Paleochannel characteristics	63	Current direction	64
Composition and source area	64	Conclusion	65
References cited	65	References cited	65
Figures		Figures	
1. Index map	31	1. Index map	51
2. Stratigraphic section	32	2. Aerial photograph of western thesis area	52
3. Stratigraphy from Gunsight Butte Member of Entrada Sandstone to Dakota Formation	33	3. Stratigraphic column	53
4. Physiographic map of southwestern Colorado Plateau	34	4. Geologic map	55
5. Map pipe location and stratigraphy, with joint roses	35	5. Bifurcation of channel B (photo)	57
6. Map outline of pipe 3	36	6. Map of channel A, segment 2	58
7. Map outline of pipe area 29	37	7. Map of channel B, segments 5, 6, 7, and 8	59
8. Map outline of pipe 35	38	8. Map of channel D, segment 6	59
9. Map outline of pipe 43	38	9. Map of channel C, segments 2 and 3	60
10. Map outline of pipe 51	38	10. Accretion ridge	61
11. Map outline of pipe 52	38	11. Erosional surface channel fill	61
12. Photograph of pipe 3	39	12. Erosional surface channel fill	61
13. Photograph of sandstone block of pipe 5	39	13. Trough cross-beds	62
14. Photograph of interior of pipe 3	39	14. Planar cross-beds	62
15. Photograph of fracture at pipe edge of pipe 26	40	15. Climbing ripples	62
16. Photograph of pipe complex 29	41	16. Scour-and-fill deposits	62
17. Photograph of thin dike complex of pipe 29	42	17. Graded bedding in trough cross-beds	63
18. Photograph of main "feeder" dikes and extensions of thin dike complex pipe area 29	42	18. Chert-cemented structure	63
19. Photograph of pebbly interior of lowermost thin dikes of pipe complex 29	42	19. Grading at base of channel A	63
20. Photograph of pipe 35	42	20. Vertical sequence of channel A	64
21. Photomicrograph of gradational edge of pipe 35	43	21. Cross section of a point bar in channel D	65
22. Photograph of base of pipe 35	43	Tables	
23. Photograph of northern face of pipe 43	43	1. Paleochannel characteristics	64
24. Photograph of sandstone and mudstone blocks at base of pipe 43	44	2. Channel composition	65
25. Photomicrograph: Thin section of interior of pipe 47	44		
26. Photograph of pipe 52	44		
27. Histogram of grain-size distribution	45		
28. Photomicrograph: Thin section of pebbly interior of pipe 3	46		
29. Photograph of converging dikes between pipes 10 and 11	47		

The Stratigraphy and Structure of the Cedar Hills, Sanpete County, Utah	67
Abstract	67
Introduction	67
Previous work	67
Acknowledgments	67
Geologic setting	68
Eocambrian to Jurassic	68
Jurassic to Cretaceous	68
Cretaceous to Eocene	68
Oligocene	68
Miocene to Recent	68
Present-day setting	68
Stratigraphy	69
Cretaceous-Tertiary	70
North Horn Formation	70
Tertiary	70
Flagstaff Formation	70
Colton Formation	72
Green River Formation	72
Tertiary volcanic rocks	73
Tertiary-Quaternary	74
Stream gravels	74
Landslides	74
Quaternary	75
Alluvium	75
Structure	75
Tectonic history	77
Economic geology	77
Summary	79
References cited	79

Figures

1. Index map	67
2. Stratigraphic column of rocks exposed in study area	69
3. Bedrock geology map	70
4. North Horn Formation	71
5. Outcrop of North Horn Formation	71
6. Outcrop of Flagstaff Formation	71
7. Colton Formation	72
8. Green River Formation	73
9. Large landslide in Big Hollow involving Colton and Green River Formations	74
10. Rounded cobbles of water-laid conglomerate	75
11. Landslide involving Tertiary volcanic rocks	75
12. Large quartzite boulder	76
13. Steplike terraces in stream gravels	76
14. View of Big Hollow	76
15. Aerial view of Water Hollow	76
16. Recent landslide in Big Hollow involving Green River Formation	77
17. Geologic map of study area and cross section in pocket	
18. Orogenic evolution of study area	78

Paleoenvironments of the Lower Triassic Thaynes Formation, near Diamond Fork in Spanish Fork Canyon, Utah County, Utah

Abstract	81
Introduction	81
Location	81
Geologic setting and stratigraphy	82
Previous work	83
Methods	84
Acknowledgments	84

Lithology	84
Sandstone	84
Red to purple sandstone	85
Orange to brown sandstone	85
Olive gray to greenish gray sandstone	85
Yellow to grayish yellow sandstone	85
Very pale yellowish green to light greenish gray sandstone	85
Siltstone	88
Brownish red to pale red and pale red purple siltstone	88
Olive to greenish gray and grayish yellow green siltstone	88
Yellow, brown, and grayish orange siltstone	89
Shale	89
Claystone and mudstone	89
Limestone	89
Mudstone	89
Wackestone	89
Packstone	90
Grainstone	90
Floatstone	90
Bindstone	90
Cyclic patterns	91
Sedimentary structures	92
Cross-bedding	93
Flaser bedding	93
Lenticular bedding	93
Paleontology	93
Occurrence and preservation	93
Body fossils	93
Crinoids	94
Echinoids	94
Conodonts	94
Foraminifera	94
Brachiopods	94
Fish fragments	95
Sponges	95
Ostracodes	95
Steinkerns	95
Bivalves	95
Gastropods	95
Algal stromatolites	96
Ichnofossils	96
Paleoenvironment	96
Paleoclimate	96
Currents and energy levels	96
Sedimentary model	96
Marine	96
Subtidal	97
Intertidal	98
Supratidal	98
Summary	98
References cited	99

Figures

1. Index map of study area	81
2. Stratigraphic column	82
3. Conodont zonation and age assignment of rocks of study area	83
4. Detailed stratigraphic section of study area	86, 87
5. Low cross-bed sets	88
6. Double-trail pascichnia	88
7. Photomicrograph: Sponge spiculate	89
8. Domichnia and vertical burrows	90

9. Mud clast with bivalve and ostracode valves	90	11. Gravity profile b-b' and 2 ½-dimensional interpretive model	112
10. Crinoid ossicles with algal and fecal pellets	90	12. Gravity profile c-c' and 2 ½-dimensional interpretive model	112
11. Photomicrograph: Grainstone	91	13. Gravity profile d-d' and 2 ½-dimensional interpretive model	112
12. Photomicrograph: Algal stromatolite	91	14. Gravity profile e-e'	113
13. Generalized representation of 3- and 5-element cycles of measured section	91	15. Gravity profile f-f' and 2 ½-dimensional interpretive model	113
14. Typical 5-element cycle in units 169 to 174	92	16. Gravity profile g-g' and 2 ½-dimensional interpretive model	113
15. Symmetrical current ripples in coarse siltstone	92	17. Gravity profile g-g' and 2 ½-dimensional interpretive model (alternative interpretation)	114
16. Undulatory to lingoid current ripples in red siltstone	92	18. Gravity profile g-g' and 2 ½-dimensional interpretive model (alternative interpretation)	114
17. Micro-cross-lamination in red siltstone of unit 89	93		
18. Lyssakid hexactinellid sponges	95		
19. Energy index of rocks of measured section	97		
20. Transgressive-regressive sequences in the Thaynes Formation	99		
A Gravity Study of the Nampa-Caldwell Area, Canyon County, Idaho			
Abstract	101	Geology of the Sterling Quadrangle, Sanpete County, Utah	117
Acknowledgments	101	Abstract	117
Introduction	101	Introduction	117
Previous work	101	Location	117
Current work	101	Previous work	117
Regional geologic setting	101	Stratigraphy	117
Structural geology of the Nampa-Caldwell area	102	Jurassic System	118
Stratigraphy	104	Arapien Shale	118
Data acquisition and reduction	104	Cretaceous System	118
Instrumentation	104	Sanpete Formation	118
Survey technique	104	Allen Valley Shale	118
Data reduction	104	Funk Valley Formation	120
Terrain corrections	105	Sixmile Canyon Formation	120
Reliability of data	105	Price River Formation	120
Gravity data analysis	105	Cretaceous-Tertiary	120
Terrain-corrected Bouguer gravity anomaly map	105	North Horn Formation	120
Third-order residual gravity anomaly map	107	Tertiary	120
Regional gravity map	107	North Horn Formation	120
Interpretation	107	Tertiary System	121
Residual gravity anomaly map—General remarks	107	Flagstaff Formation	121
Profile modeling	111	Colton Formation	121
Gravity profile a-a' and interpretive model	111	Green River Formation	121
Gravity profile b-b' and interpretive model	111	Crazy Hollow Formation	122
Gravity profile c-c' and interpretive model	112	Quaternary System	122
Gravity profile d-d' and interpretive model	112	Structural geology	123
Gravity profile e-e'	113	East region	123
Gravity profile f-f' and interpretive model	113	Faults	123
Gravity profile g-g' and interpretive model	113	Diapir	123
Summary and conclusions	114	Unconformities	123
References cited	114	Central region	124
Figures			
1. Index map	101	Diapir	124
2. Topographic map	102	Unconformities	125
3. Preliminary geologic map of the Nampa-Caldwell area	103	West region	126
4. Stratigraphic column	104	Faults	126
5. Terrain-corrected Bouguer gravity anomaly map	106	Diapir	126
6. Instrument-performance record for time data	107	Unconformities	127
7. Third-order polynomial model	108	Geologic history	127
8. Third-order polynomial residual gravity anomaly map	109	Jurassic Period	127
9. Third-order polynomial residual gravity anomaly map	110	Cretaceous Period	127
10. Gravity profile a-a' and 2 ½-dimensional interpretive model	111	Tertiary Period	129
		Economic geology	129
		Conclusions	129
		Acknowledgments	130
		Appendix	130
		References	135

Figures

1. Index map	117	16. Angular unconformity at south end of San Pitch Mountains	125
2. Aerial view of Sterling Quadrangle	118	17. Unconformity: Green River Formation on Arapien Shale	126
3. Stratigraphic column	119	18. Unconformity: Quaternary gravels on overturned Arapien Shale	126
4. Geologic map and cross sections	in pocket	19. North Horn Formation beds overturned	127
5. Photomicrograph: Charophytes and gastropod fragments in freshwater limestone	121	20. Upright beds caught in lower units folded over by diapir	127
6. Photomicrograph: Oncolite	121	21. Syncline in North Horn Formation	127
7. Photomicrograph: Brecciated limestone	122	22. Comparison of structural configuration proposed in this study and that proposed by Gilliland (1963)	128
8. Oncolite conglomerate facies	122	23. Schematic representation of structural development of Sterling Quadrangle	130, 131
9. Photomicrograph: Clasts in Quaternary gravels	123		
10. Locations and elevations of Quaternary gravels	123		
11. Large landslide in Forbush Cove	124		
12. Landslide in Green River Formation	124		
13. Three regions in Sterling Quadrangle	124		
14. West flank of Wasatch Monocline and east flank of anticline	125		
15. Double angular unconformity at mouth of Sixmile Canyon	125		
		Publications and maps of the Geology Department ...	137

Exhumed Paleochannels in the Lower Cretaceous Cedar Mountain Formation near Green River, Utah*

DANIEL R. HARRIS
Utah International, Inc.
20 West 2950 South
Salt Lake City, Utah 84115

ABSTRACT.—The Cedar Mountain Formation southwest of Green River, Utah, contains four of the longest known Lower Cretaceous exhumed fluvial channels on the Colorado Plateau.

Sediment transport direction was from the west-southwest, where Permian beds and possibly other Paleozoic units were being eroded from the Sevier uplift. Some chert pebbles from the paleochannel conglomerates were derived from Permian rocks. They contain fragments of bryozoans, echinoderms, brachiopods, and monaxial sponge spicules.

The paleochannels range in length from 4.5 km to 8 km where a maximum width of 224 m was exhibited on channel C. Channel B, segment 5, and channel C, segment 6, both exhibit a bifurcation in the main channel course.

The paleochannels can be divided into two distinctive parts: point-bar and channel-fill deposits. Point-bar deposits are found on the inside of channel inflections and exhibit accretion ridges with a dip perpendicular to the sediment transport direction of the channel fill. Channel fills rise 1.5 m to 5 m above the point-bar deposits and commonly exhibit scour-and-fill structures throughout their vertical sequence.

According to calculated values made with formulae derived by Schumm (1963, 1972), the four paleochannels were determined to have shallow gradient, averaging 0.28 m per km, with a maximum annual discharge rate in channel C of 600 m³/sec.

INTRODUCTION

Four long, linear, conglomeratic sandstone-capped ridges and numerous shorter ridge segments are exposed in the badlands of the Cedar Mountain Formation southwest of Green River, Utah (fig. 1). They are exposed as some of the longest-known such ridges on the Colorado Plateau. Long linear ridges observed on the Colorado Plateau have originated from various types of rocks or structures: inverted valleys, dikes, fault escarpments, resistant upturned beds, and resistant fluvial deposits. Because of the present-day arid climate and limited plant cover over much of the Colorado Plateau, thick, masking accumulation of soil has been prevented. Because of deep and intricate erosion by streams of the Colorado Plateau, excellent, three-dimensional study of sedimentary bodies like these conglomerate-sandstone ridges is possible.

Location

The conglomeratic sandstone-capped ridges occur in sections 19 to 29 and 32 to 34, T. 22 S, R. 15 E, in Emery County, Utah, on the Tidwell Bortoms and Green River, Utah, 30-minute topographic quadrangles. The ridge crests stand at an elevation of approximately 1,370 m.

Eastern sections of the ridges are located approximately 11 km southwest of Green River, Utah. They are accessible via Canyonlands Road, a graded, dirt county road that leads southward from the center of the community of Green River, Utah. This road intersects the eastern half of one of the main ridges 2 km north of Horse Bench Reservoir. From that point segments of the same ridge and another more southerly one are accessible via old claim-assessment roads.

The western ridges are located 5 km southeast of the junction of Interstate 70 and Utah 24, west of Green River, Utah, and north of Hanksville, Utah (fig. 2). Immediate access to the capped ridges is provided by an unmaintained dirt road which heads southeastward from the head of Jessies Twist on the old paved road that formerly connected Green River and Hanksville. This dirt road intersects the west end of the northernmost ridge approximately 2 km southeast from Jessies Twist. Several unimproved claim-assessment roads can be followed from here to nearly any conglomeratic sandstone ridge in the western part of the study area.

Previous Work

Lower Cretaceous beds on the Colorado Plateau were earlier described by Coffin (1921, p. 97) in southwestern Colorado. He proposed the term "post-McElmo" for several units between the McElmo and the Dakota Formations. These units were later renamed the Burro Canyon Formation by Stokes and Phoenix (1948) from exposures in Burro Canyon, San Miguel County, Colorado. Stokes (1944, p. 966-67) earlier, however, used the Cedar Mountain Formation to refer to variously col-

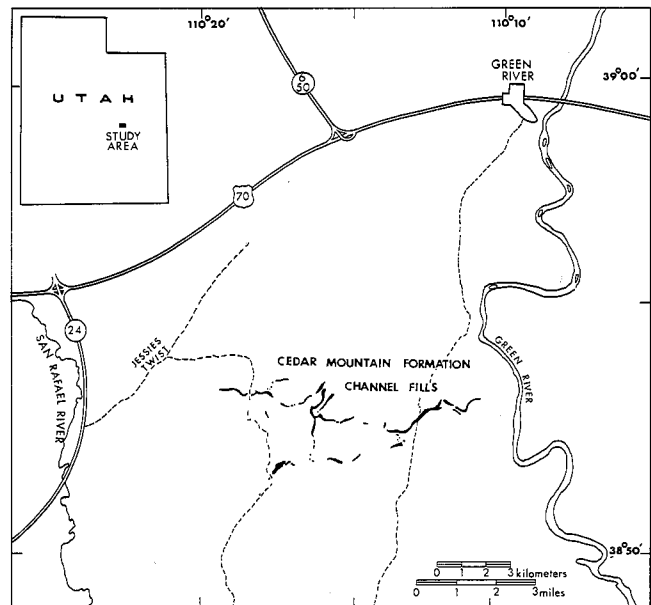


FIGURE 1.—Index map.

*A thesis presented to the Department of Geology, Brigham Young University, in partial fulfillment of the requirements for the degree, Master of Science, August 1979. Thesis chairman: J. Keith Rigby.

ored Lower Cretaceous mudstone beds between the Buckhorn Conglomerate and the Dakota (?) Sandstone. The mudstone sequence is at nearly the same stratigraphic position as the Burro Canyon Formation. The type section and locality of the Cedar Mountain Formation are on the southwest flank of Cedar Mountain, Emery County, Utah, immediately north of Buckhorn Reservoir. Stokes (1944, p. 989) recommended that the Lower Cretaceous Buckhorn Conglomerate and the Cedar Mountain Formation be combined in the Cedar Mountain Group. However, upon subsequent observations of the Buckhorn Conglomerate, Stokes (1952, p. 1774) realized that it was discontinuous and generally too thin to map. He then recommended that the Buckhorn Conglomerate be considered only as the basal member of the Cedar Mountain Formation.

Because the Burro Canyon Formation and the Cedar Mountain Formation are approximately time-equivalent units, the lower Cretaceous varicolored mudstones east of the Colorado River are considered to be Burro Canyon Formation and those west of the river within the Cedar Mountain Formation. These outcrops of concern in the present study are included in the Cedar Mountain Formation. According to Stokes (1952, p.

1774) only in outcrops near Dewey, Grand County, Utah, are the two formations in physical continuity.

The Burro Canyon and Cedar Mountain Formations correlate with the Kelvin Formation in north central Utah (Trimble and Doelling 1978, p. 69). Trimble and Doelling (1978, p. 68-72) recently described the Cedar Mountain Formation in their study of uranium and vanadium deposits in the San Rafael mining area, in Emery County, Utah, a short distance northwest of the present study area. They included several measured sections of the Cedar Mountain Formation and provided a general description of the various units within the formation.

The linear conglomeratic sandstone lenses in the Cedar Mountain Formation have received little detailed attention. Only a few geologists have mentioned them. In a study of the Dakota Group of the Colorado Plateau, Young (1960, p. 158-69) briefly described some of the characteristics of the channel deposits and illustrated their areal extent. Stokes (1961, p. 168-69), in a paper on fluvial and aeolian processes, showed an areal photograph and related photographs of the conglomeratic sandstone channel fills in parts of the Cedar Mountain Formation southwest of Green River, Utah.

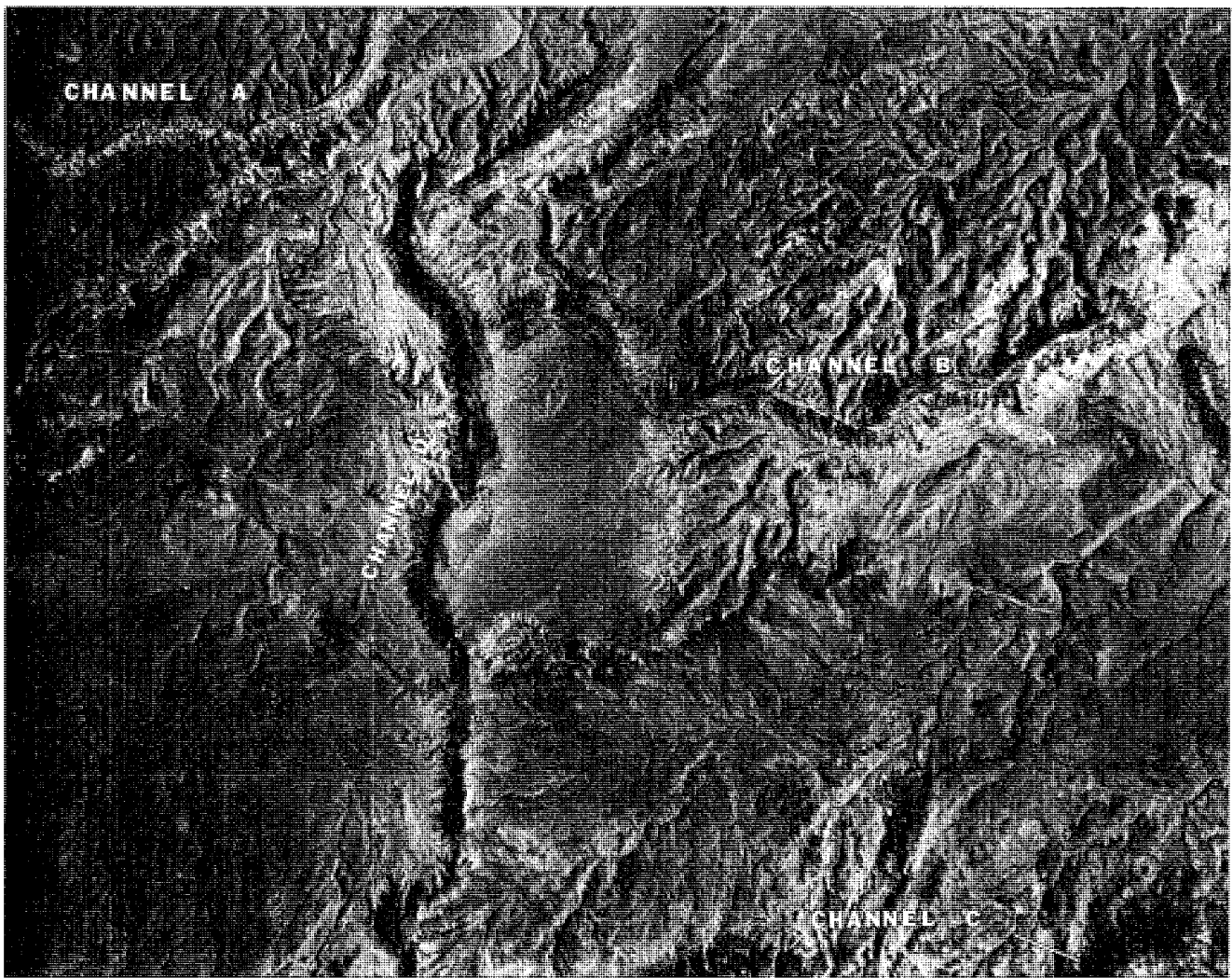


FIGURE 2.—Aerial photograph at west end of study area, showing parts of channels A, B, C, and D. Base of photograph is approximately 3.5 km.

Derr (1974) described exhumed fluvial channel fills in the Brushy Basin Member of the Morrison Formation. These Morrison channels are located 8 km northwest of the study area, immediately east of the junction of Interstate 70 and Utah 24. Derr's study documented three short channel-fill segments, two of which are genetically related and were considered to be point-bar deposits. The third channel fill is an isolated segment and has bedload fluvial characteristics.

Methods

Mapping and fieldwork were conducted during the summer and fall of 1978 and in the winter of 1979. Current directions from cross-bedding and dips on accretion ridges were determined by the use of a Brunton compass. A 50-m fiberglass tape was used to measure thickness and widths of the conglomeratic sandstone ridges. Topographic maps and aerial photographs were used in mapping the study area and for the preparation of plan view illustrations. Twenty thin sections were prepared from several rock samples to determine composition for the ridges.

Acknowledgments

The writer wishes to thank J. Keith Rigby who served as thesis chairman and Jess Bushman who served as a committee member. Thanks are given to my wife, Margie, for typing, and to my father, Wayne, for fieldwork assistance and financial help. Appreciation is extended to Brigham Young University, Geology Department Research Fund, for financial assistance for part of the fieldwork.

GEOLOGIC SETTING

Continental sediments which produced the sandstone and conglomerate in the Cedar Mountain Formation and related sediments were derived from the Sevier geanticline (Stokes 1972, p. 25). The Sevier geanticline was an orogenic belt that began to rise and become a positive area in Late Jurassic time. It was during this time that stream-laid sands and gravels were deposited east of the Sevier Highlands on floodplains west of the advancing Cretaceous sea. Deposition of these stream-laid sediments continued from Late Jurassic (Morrison Formation) to Early Cretaceous time when the Cedar Mountain Formation accumulated. According to Trimble and Doelling (1978, p. 69) the fluvial and lacustrine environments that were responsible for the Brushy Basin Member of the Morrison Formation are similar to those that produced the Cedar Mountain Formation.

The last epicontinental sea that covered parts of Utah occupied the eastern part of the state in Late Cretaceous time. This seaway extended northwestward from the Texas area into eastern Utah (Hintze 1973, p. 67). The Cretaceous sea was limited in its westward spread by highlands and deltaic deposits of the Sevier orogenic belt. Cedar Mountain beds were deposited along the western margin of the Lower Cretaceous phase of the marine invasion and were buried by Late Cretaceous marine clays and mudstones in the later phase of the invasion.

Today the area of study lies within the northern end of the Canyonlands section of the Colorado Plateau, a short distance east of the eastern flank of the San Rafael Swell. This general area, according to Trimble and Doelling (1978, p. 77), shows influences of three tectonic units: the San Rafael Swell, the Uinta Basin, and the Paradox fold and fault belt. Rocks in the thesis area dip 3-5° to the northeast into the southern part of the Uinta Basin.

STRATIGRAPHY

All exposed consolidated rock units in the thesis area are sedimentary rocks deposited during the Mesozoic Era (fig. 3). The oldest rock unit of concern in the present study is the Ju-

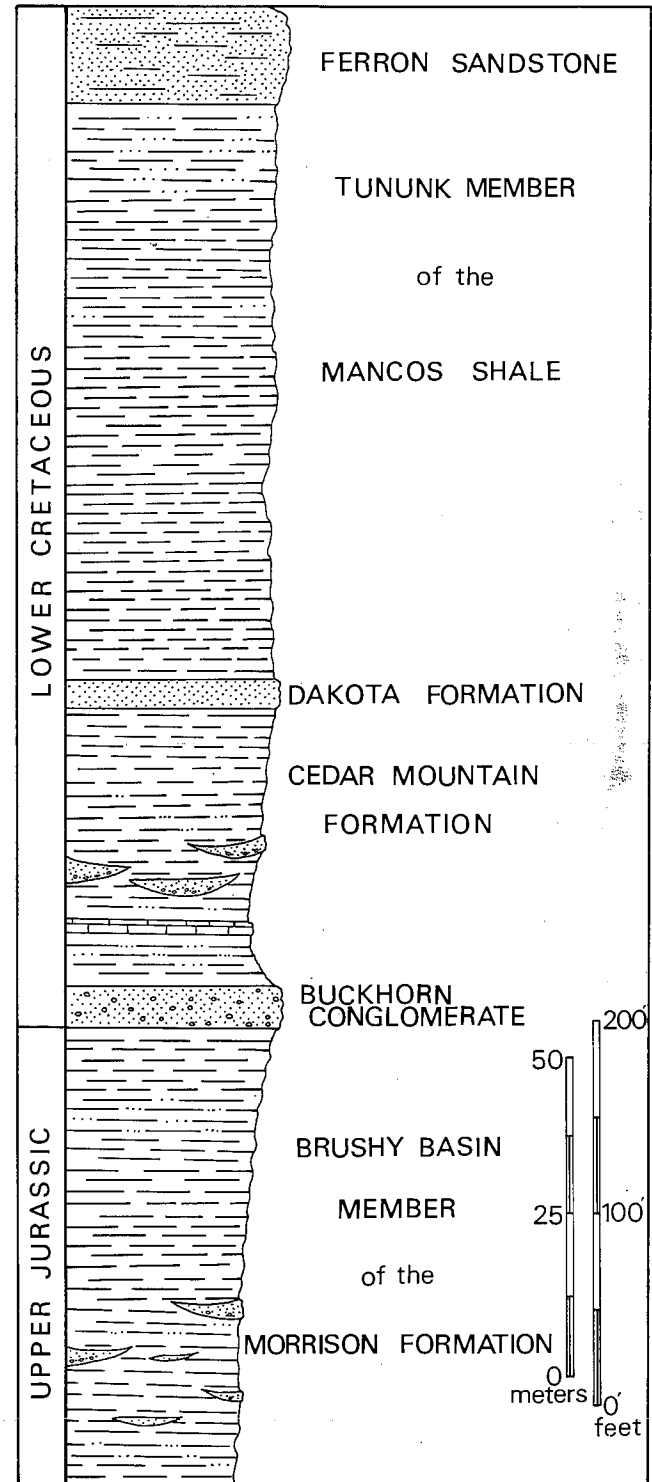


FIGURE 3. Stratigraphic column.

rassic Morrison Formation. The Brushy Basin Member of the Morrison Formation is exposed in a belt south of the Cedar Mountain beds in the southern part of the thesis area (fig. 4). The Brushy Basin Member is overlain by the Lower Cretaceous Cedar Mountain Formation which includes the basal Buckhorn Conglomerate and an overlying Cedar Mountain shale member. It is with the shaly upper Cedar Mountain beds that the thesis is primarily concerned. The Dakota Formation is exposed as discontinuous lenses above the Cedar Mountain Formation and is overlain by the Tununk Member, the basal shale member of the Mancos Shale. The youngest unit exposed in the immediate thesis area is the Ferron Sandstone Member of the Mancos Formation. Because of a gentle northward dip, younger rock units in the thesis area are progressively exposed toward the north.

Morrison Formation

The Morrison Formation has four regionally recognized members: Salt Wash, Recapture, Westwater Canyon, and Brushy Basin Members. Only the Brushy Basin and the Salt Wash Members of the Morrison Formation are recognized in the Green River-San Rafael area (Hintze 1973, p. 156; Trimble and Doelling 1978, p. 62). Only the Brushy Basin Member is exposed in the thesis area although Salt Wash beds crop out farther south and northwest. Outcrops of Brushy Basin beds form an irregular badland-margined cuesta south of the Cedar Mountain Formation.

According to Trimble and Doelling (1978, p. 62), the Brushy Basin Member is composed mainly of claystone, mudstone, siltstone, and shale. This member, perhaps more than any other, is typically varicolored with bands of reds, purples, grays, and gray greens. It weathers to a popcornlike surface, produced by weathering of the interbedded bentonitic argillaceous beds, and forms rounded hills and intricately carved badlands.

The Brushy Basin Member, like most other units in the Morrison Formation, was formed by mainly fluvial processes that produced extensive floodplains during Late Jurassic (Stokes 1944, p. 987). Some lake deposits also accumulated on part of the floodplains. The contact of the Brushy Basin Member of the Morrison Formation with the overlying Cedar Mountain Formation marks the boundary between the Jurassic and Cretaceous Systems, according to Stokes (1952, p. 1769).

Cedar Mountain Formation

The Cedar Mountain Formation crops out in central, eastern, and northeastern Utah. Some of the most prominent exposures are those located in the type area and elsewhere around the San Rafael Swell.

The Cedar Mountain Formation consists of two members, the basal Buckhorn Conglomerate and an overlying unnamed shale member, in which the conglomerate lenses of the present study lie. The Buckhorn Conglomerate is thickest to the north around the San Rafael Swell, with a maximum thickness of 9 m, and pinches out toward the southwest. The shale member of the Cedar Mountain Formation has an average thickness of 49 m but varies between 44 m and 56 m in the eastern San Rafael Swell district (Trimble and Doelling 1978, p. 69), a few miles west of the present study area.

The contact between the Cedar Mountain Formation and the Brushy Basin Member of the Morrison Formation is marked in many areas by the Buckhorn Conglomerate, which lies disconformably over the Brushy Basin beds. The Buckhorn Conglomerate is composed of sand- and pebble-size fragments

of chert, quartzite, and other terrigenous material in the area of study and becomes a tan gritstone in the southernmost exposures in the San Rafael district (Trimble and Doelling 1978, p. 68).

Many workers have pointed out the similarities between the Brushy Basin Member of the Morrison Formation and the younger shale member of the Cedar Mountain Formation. One of the more obvious features is the colored banding of both units, but the Cedar Mountain Formation shows more faded or ashy-appearing outcrops and banding is less prominent. Similarities between the Brushy Basin Member of the Morrison Formation and the Cedar Mountain Formation, according to Stokes (1944, p. 981), possibly may have been produced from reworking of Brushy Basin shales into the Cedar Mountain Formation.

The shale member is composed principally of siltstone, shale, and mudstone, with minor sandstone and limestone. According to Trimble and Doelling (1978, p. 68), the siltstone, shale, and mudstone are commonly bentonitic and form the bulk of the member. In some areas, the shale member forms intricate badlands, but generally it erodes to soft gentle hills where unprotected by overlying resistant beds.

Fluvial and lacustrine processes similar to those that deposited the Brushy Basin Member of the Morrison Formation continued into Lower Cretaceous time and deposited the Cedar Mountain shale member. Evidences of fluvial environments are preserved in the Cedar Mountain shale as conglomeratic sandstone channel segments. These conglomerate lenses are fairly extensive at several horizons in the area of study (Young 1960, p. 158-65; Stokes 1944, p. 967). Many of the conglomerate sandstone deposits now stand as elongate ridges because the enclosing softer floodplain mudstones were eroded away. Details of these conglomerate lenses will be presented later.

The Cedar Mountain Formation is considered to be Lower Cretaceous, on the basis of fossils reported from the upper part of the formation by Stokes (1944, p. 966) and Katich (1951).

Dakota Formation

The Dakota Formation is a thin, discontinuous sandstone in the thesis area (fig. 4). It is largely missing in the area between the east flank of the San Rafael Swell and the Green River. Scablike remnants mapped by Trimble and Doelling (1978, p. 72) crop out immediately north of the linear conglomerate ridges of the thesis area, at the southern edge of a subsequent valley carved in the Mancos Shale. The areal extent of outcrops of the Dakota Formation is less than 8 ha (20 acres) in the area of primary concern (fig. 4). The Dakota Formation lies disconformably upon the underlying Cedar Mountain Formation and represents fillings of shallow scours. The upper contact with the Mancos Shale varies from gradational to disconformable.

The Dakota Formation is the basal deposit of the transgressive Mancos sea (Lawyer 1972, p. 90; Hintze 1973, p. 67; Trimble and Doelling 1978, p. 73). In the general area of this study the Dakota Formation appears to be fluvial (Trimble and Doelling 1978, p. 73).

Mancos Formation

The Mancos Formation overlies the Dakota Formation (fig. 4) and, in many areas surrounding the San Rafael Swell, also locally disconformably overlies the Cedar Mountain Formation. The Mancos Shale weathers to low ridges and mounds.

Several tongues of interfingering sandstone and shale were deposited near the oscillating western shoreline during Mancos

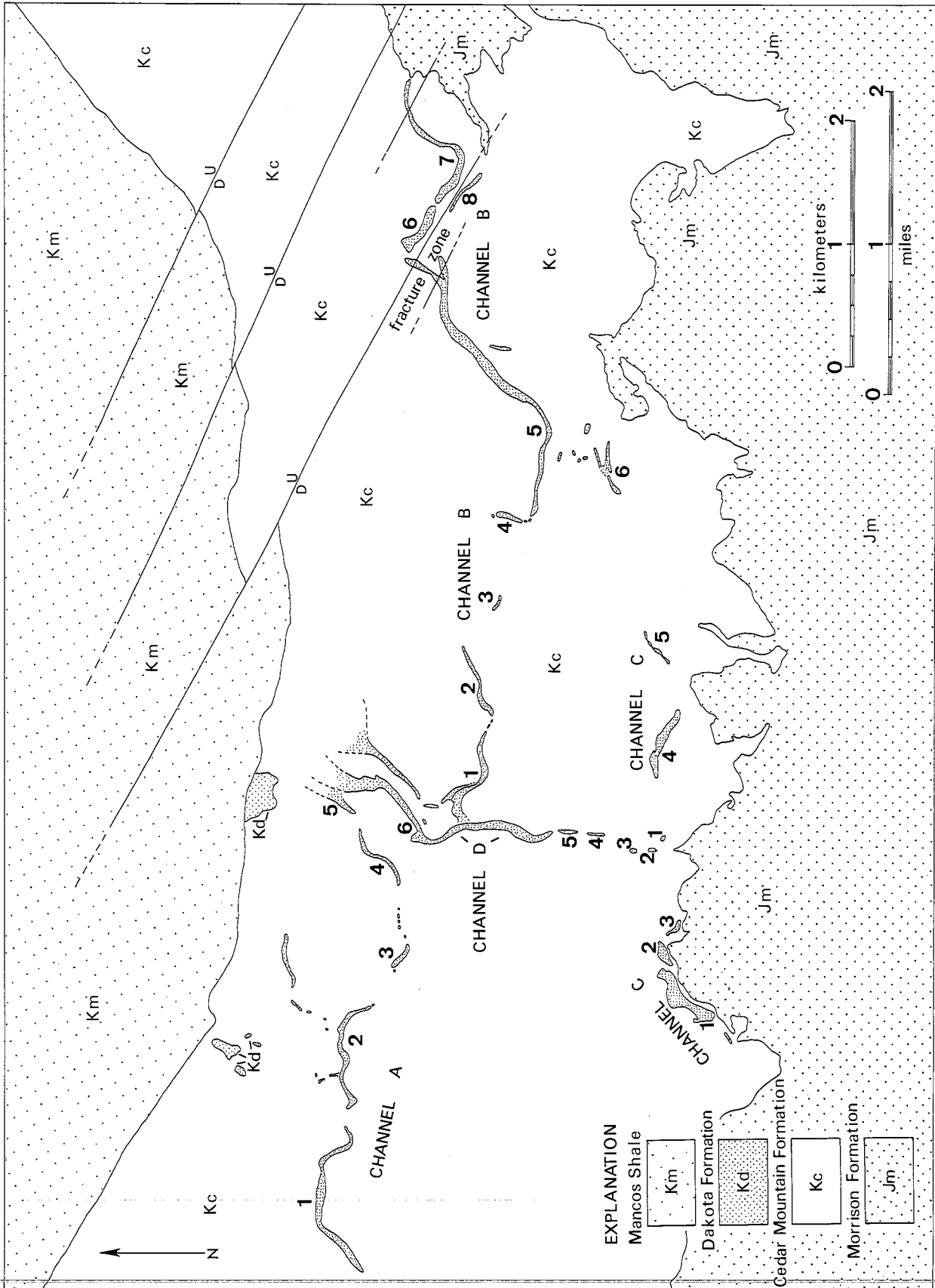


FIGURE 4.—Geologic map showing current direction toward increasing channel segment numbers.

time. Characteristic eastward regressions are represented by the Ferron and Emery Sandstone Tongues, and westward transgressions are represented by intervening shale tongues of the Mancos Shale.

The Mancos Formation crops out north of the Cedar Mountain belt. The Ferron Sandstone Member forms a cuesta which extends east-west across the northernmost part of the area of study. The Ferron Sandstone cuesta is offset by several normal faults that strike northwestward through the escarpment.

CHANNEL CLASSIFICATION

The conglomeratic sandstone-capped ridges in the Cedar Mountain Formation are similar to the conglomeratic sandstone and sandstone deposits found in the Salt Wash Member of the Morrison Formation. The Morrison Formation has long been interpreted as an extensive fluvial accumulation (Mook 1916; Baker, Dane, and Reeside 1936; Stokes 1944). Since the Morrison and Cedar Mountain Formations are a result of similar environments, as concluded by Trimble and Doelling (1978, p. 69), the conglomeratic sandstone-capped ridges in the Cedar Mountain Formation are also probably of fluvial origin. Stokes (1944, p. 967; 1961, p. 166-69) and Young (1960, p. 158-65) briefly investigated the conglomeratic sandstone-capped ridges and from their studies concluded that they are predominately fluvial in origin and represent exhumed channel fills.

The conglomeratic sandstone ridges in the Cedar Mountain Formation are termed *paleochannels* or simply *channels*. According to Stokes (1961, p. 165) the term *channel* refers to a body of clastic material, regardless of size and shape, generally sandstone and/or fine conglomerate, originally deposited by rapidly flowing water in an ancient stream course, which has internal structures indicating the direction of sediment transport.

Outcrops of the Cedar Mountain Formation conglomeratic sandstone-capped ridges consist chiefly of paleochannel fills that are resistant enough to be exposed in various stages of exhumation.

Observations on channel dimensions, patterns, sedimentary structures, lithology, and vertical sequence of rock bodies in the thesis area will be discussed in the following sections.

CHANNEL DIMENSIONS

The exhumed paleochannel fill deposits of the thesis area occur as several segments of four major, but discontinuous, channel fills (fig. 4). A *channel segment*, as the term is used in this paper, is any conglomeratic sandstone channel fill body exceeding 30 m in length. Sandstone bodies less than 30 m long, which appear to be in place, are referred to as *channel remnants*. The channel segments commonly occur as plano-convex lenses of various lengths and widths. Some identified segments are as little as 5 m wide but expand to 224 m across in the southern part of the thesis area.

Three channel-ridges extend approximately 12 km east and west parallel to the Cedar Mountain Formation outcrop belt and lie within a strip approximately 5 km wide (fig. 4). A fourth and shorter channel trends generally north-south across the outcrop belt although the northernmost part swings to the northeast.

Originally the channel fills were surrounded and covered by softer floodplain shale and siltstone of the Cedar Mountain Formation, but now nearly all the floodplain material has been eroded away from the sides of the channel fills and intervening areas. The channel fills rest on top of protected older Cedar

Mountain shales and siltstones and have an average local relief of approximately 18 m.

Channel A

Channel A (fig. 4) lies in the northwestern part of the thesis area, approximately 3.2 km southeast from Jessies Twist. Channel A has been divided by erosion into 5 segments, separated by as little as 128 m or as much as 643 m. The channel has a maximum preserved length of 4.5 km and trends east-west. The maximum exposed width is at the west end of segment 2, where it expands to approximately 81 m (fig. 4). The narrowest point of the channel fill is located between segments 3 and 4 where five channel remnants stand. The westernmost remnant is 7.6 m to 9 m wide.

The longest preserved segment of channel A is segment 1 (fig. 4), which is approximately 1 km long. It stands at the westernmost end of the study area. The western end of segment 1 terminates abruptly and overlooks the Brushy Basin-produced escarpment in the Morrison Formation.

The south side of segment 2 of channel A, approximately 96 m east of its western tip, has a maximum thickness of 9 m. On the opposite side of this segment the fill is only 2 m thick. Thicknesses of all channel segments throughout the study area pinch and swell, and in some areas thickness is impossible to measure because of enclosing floodplain material and younger soil cover.

Two earlier channel segments have been cut across and truncated at approximately 90° degrees by channel A, segment 2, on the north side of the channel (fig. 4). Continuations of the two older channels have been lost on the south side of segment 2 because of erosion.

Channel B

Channel B is the longest of the four major paleochannels in the study area. It measures approximately 8 km along a straight line from its westernmost preserved point to the eastern end of the fill. Channel B is 10 km long, as measured along its course. Segment 5 of channel B (fig. 4) is the longest continuous segment in the thesis area. It extends east-west for 3 km. The thickest point on the channel is in the eastern part of segment 5, on the south side, where the conglomeratic fill is 11 m thick. The widest point is at the northwestern end of segment 6, where the preserved channel is 128 m wide.

The westernmost end of channel B is truncated by channel D. Any more projected extensions of channel B to the west have been removed by erosion.

Several channel remnants stand between segments 1 and 2 and segments 3 and 4. It is at these points that the preserved channel fill narrows to a width of 4.6 m. Access to these channel remnants is difficult because of their vertical walls and the soft, steeply eroded shales beneath.

The eastern end of segment 5 bifurcates, with the more narrow fill trending at an angle to the main wider course. The main fork of the channel trends N 35° E, and the narrower segment trends N 80° E (figs. 4, 5). These two channel fills become parallel along segment 8.

The easternmost end of segment 7 comes to an abrupt end in a fault zone approximately 38 m above the Brushy Basin escarpment which overlooks the Green River.

Channel C

Channel C is the southernmost paleochannel, running parallel to the edge of the Brushy Basin escarpment. The max-

imum length of the channel is 6.4 km, and it trends N 80° E. Segment 1 includes the maximum exposed width and thickness of any fill found in the thesis area: Approximately 224 m across at midlength and 15 m thick at the southern point of the segment.

Approximately 1.6 km separate segments 3 and 4 and segments 5 and 6. These are the greatest distances separating identified related channel segments in the thesis area.

Segment 6 also shows bifurcation of the channel and is similar to the eastern end of segment 5 of channel B. These two courses of channel C trend N 70° E and N 89° E at their easternmost extensions.

Channel D

Channel D is separated into six discontinuous segments (fig. 4). Segment 6 is 1.9 km long and is the longest portion of the channel. It trends generally north-south, but the northern part swings to the northeast and disappears beneath younger beds in a hill. Immediately south of the hill the channel widens to approximately 128 m, nearly twice the average width of the channel remnant to the south. It narrows to 39.6 m wide at its southern termination, immediately above the Brushy Basin escarpment. The average thickness of segment 6 is consistently about 7.6 m along the western edge of the channel.

CHANNEL PATTERNS

Channel patterns, according to Leopold and Wolman (1957, p. 39), are used to describe the plan view of a river as it would be seen on aerial photographs. Leopold and Wolman (1957) have classified river channel patterns into three major categories: meandering, straight, and braided. Classifications of streams and other natural phenomena, according to Schumm (1963, p. 1089), are arbitrary, and attention is thus focused on the extreme end members or more naturally occurring state of the natural phenomena. In the classification of river channel patterns the very sinuous stream, the straight stream, and the stream that contains islands are generally studied, and transitional patterns are neglected. Such a conclusion is supported by

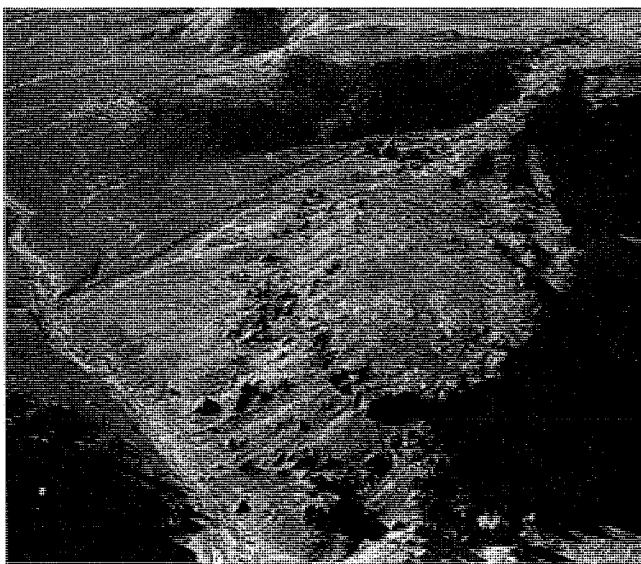


FIGURE 5.—Oblique aerial photograph of bifurcation of the channel on the east end of channel B, segment 5.

Leopold and Wolman (1957, p. 59), who conclude that transitional channel patterns do exist and show a continuum of channel patterns. Schumm (1963) further divided Leopold and Wolman's (1957) meandering and straight channel patterns into five classes. They are, in terms of decreasing sinuosity, tortuous, irregular, regular, transitional, and straight. Since there is no demarcation existing between the types of river patterns, Schumm (1963, p. 1090-91) defined limits of patterns by a measure of sinuosity (ratio of channel length to valley length) and arbitrarily assigned each of the preceding classes to a specific range of sinuosities.

Stream patterns described in terms of sinuosity have been used by Lane (1957) and by Leopold and Wolman (1957). Moody-Stuart (1966, p. 1102) added a braiding factor to Schumm's channel pattern classification. They used the term *low sinuosity* to replace braided or straight streams because the term *braided* has been used on stream patterns from meandering rivers with a few islands to highly anastomosing glacial outwash streams. Moody-Stuart (1966, p. 1102) also used the braiding index of Brice (1964) and sinuosity ratios to develop a new classification. This means a high-sinuosity river with a braiding index of zero is simply a "high-sinuosity river". Variations can then be described between high- and low-sinuosity rivers when combined with a braided index.

Braided and meandering streams, according to Leopold and Wolman (1957, p. 59), are very different but represent end members in an uninterrupted range of channel patterns. River braiding is characterized by division around alluvial islands or the anastomosing of channels by bars of alluvium (Brice 1964, p. 27). According to Coleman (1969, p. 145), one alluvial island is sufficient to classify a channel as braided, but generally several islands are found between channel banks. Meandering channels expressed on plan view show more or less regular and repeated inflections in the channel patterns, with point-bar deposits on the inside of the channel inflection.

Natural channels and experimental flume channel studies exhibit alternating pools and riffles or shallow reaches in virtually all types of channel patterns. In meandering streams, pools are located very near the concave bank, generally opposite deposits of lateral accretion. Channel areas between the points of maximum inflection of meander bends are generally straight and are called reaches (Coleman 1969, p. 150).

Meandering and braided channels are easily found and illustrated from the field, but straight channels, according to Leopold and Wolman (1957, p. 53), are rare among natural rivers and may really be nonexistent. Many channels, no matter in what classification, tend to have short segments or reaches that may be considered straight. A generalization most workers agree upon is that channel reaches which are straight for a distance exceeding ten times the channel width are rare.

Paleochannel patterns in the study area exhibit regular bends or inflections along each of the four major channels. Bends occur as both smooth arcuate reaches and elbow bends ranging between 90° and 150°. The channels do not form large meander loops like those exhibited along the lower reaches of the Mississippi River near New Orleans and along the Green River in Wyoming and Utah. The Cedar Mountain channels tend to show broad bends of low sinuosity, amplitude, and wavelength. Straight channel reaches are exhibited in channels A, B, and D, but channel C exhibits arcuate patterns in all segments.

Braiding does not appear to be expressed in any of the preserved segments in the study area. According to Shelton and Noble (1974, p. 742), the Cimarron River at Perkins, Okla-

homa, resembles both a meandering stream at bank-full stage and a braided stream at low-flow stage. As Russell (1954, p. 366) pointed out, braided and straight reaches both exist in the Meander River in Turkey, where the term *meandering* was derived. Possible periods of braiding may have existed in channels of the Cedar Mountain Formation, but the four major paleochannels of the thesis area, as they are preserved today, appear to have been the result of meandering streams.

Sinuosity

Schumm (1963, p. 1090-91; 1977, p. 115) developed a classification of five channel patterns from a study of sinuosity of alluvial rivers of the Great Plains. These patterns range from a sinuosity ratio of the straightest channel—with only slight irregularly repeating bends and a ratio of 1.05—to the opposite extreme—a highly sinuous stream, with a ratio of 2.1. The low-sinuosity stream study by Schumm appears to best represent the channel patterns in the study area. The channel patterns are more or less irregular to regularly repeating meander bends. The meander bends appear to be flattened and somewhat deformed. Smooth, sinuous, systematically repeating meander loops are absent.

Sinuosity ratios of the four major paleochannels in the study area range between 1.2 and 1.5, which would classify them as low-sinuosity, transitional to regular channel patterns. Rivers that show similar channel sinuosity patterns are the South Loup River near St. Michael, Nebraska, with a ratio of 1.5; and the North Fork of the Republican River near Benkelman, Nebraska, with a ratio of 1.2.

POINT-BAR AND CHANNEL-FILL DEPOSITS

Aerial photographs of the four major paleochannels display areas of short arcuate ridges on the surface of the channels. They were produced by the lateral accretion of sediment and are called point-bar deposits, found on the inside of channel bends. They appear to be regularly spaced along channels A, B, and D (figs. 6, 7, 8). Because of extensive erosion of channel C, it is impossible to determine regularity in point-bar spacing (fig. 9). The lower relief of the point-bar deposits as compared

to fillings of the reaches may be due to more active erosion on the dipping point-bar beds, as compared to the more horizontal beds in the channel fills.

Point-Bar Deposits

Point-bar deposits are found on all four major paleochannels on the concave side of channel inflections which generally occur at regular intervals. According to Allen (1965, p. 115), construction of point-bar deposits is connected with the pattern of water flow in a curved channel. Leopold and Wolman (1960) summarized that flow pattern in a curved channel is helicoidal, and surface water is higher on the outside of the concave bank. In the curve portion of a stream there is a downstream velocity component and a weaker sideways component. The sideways velocity has two components, one at the water surface toward the outer bank and one at the stream bed towards the convex bank over the gently shoaling point bar (Allen 1965, p. 116). Because of the helicoidal flow patterns, material eroded from the steep outer bank will tend to be deposited downstream on the next point bar. The mechanisms responsible for the accumulation of a point bar, according to Allen (1965, p. 116), are cross-channel bed flow and a decline in flow intensity toward the convex bank.

Point-bar deposits found in channels B, C, and D exhibit coarser-grained sediments than the sand-size material in the point bars of channel A. Coarse sediments in the point bars of channels B, C, and D regularly fine upward but appear to be irregular in the channel fills. Allen (1965, p. 116) referred to Fisk (1947) and Leopold and Wolman (1960), who concluded that some point bars with coarse sediments are produced by more rapid lateral bottom flow which tends to carry coarse sediments from the channel deeps to relatively high positions on the point bar.

Most of the point-bar deposits in the area of study exhibit arcuate ridges with dips perpendicular to the direction of the major channel flow (fig. 10). Dips on the accretion ridges range from 1° to 40°.

The point-bar deposits of channels A, B, C, and D generally have low relief, they do not form steep vertical walls, and

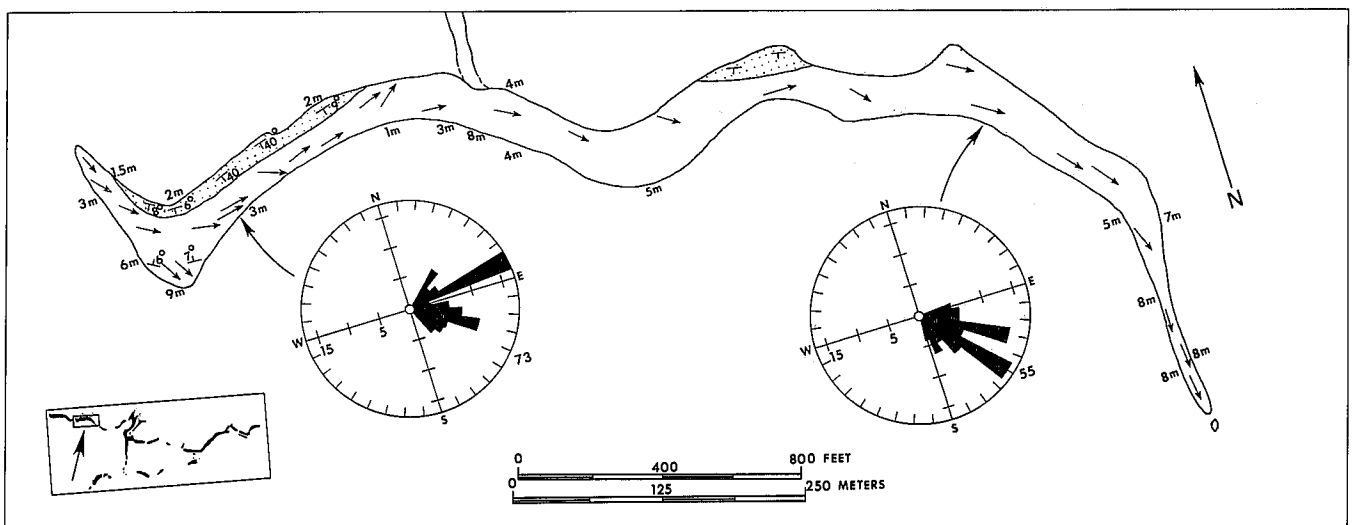


FIGURE 6.—Map of channel A, segment 2. Rose diagrams show sediment transport direction along channel segments. Number immediately below and to right of rose diagrams is number of directional features measured. Stippled areas represent point-bar deposits.

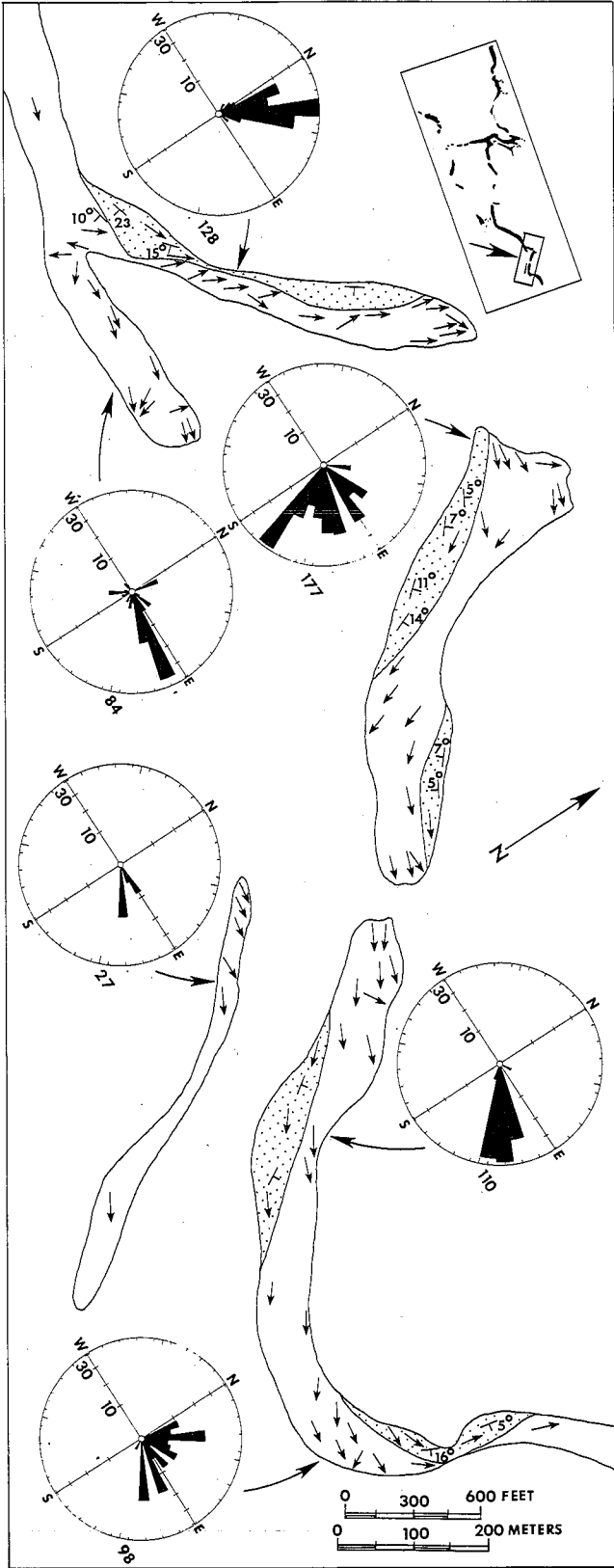


FIGURE 7.—Map of channel B, segments 5, 6, 7, and 8. Note bifurcation of segment 5.

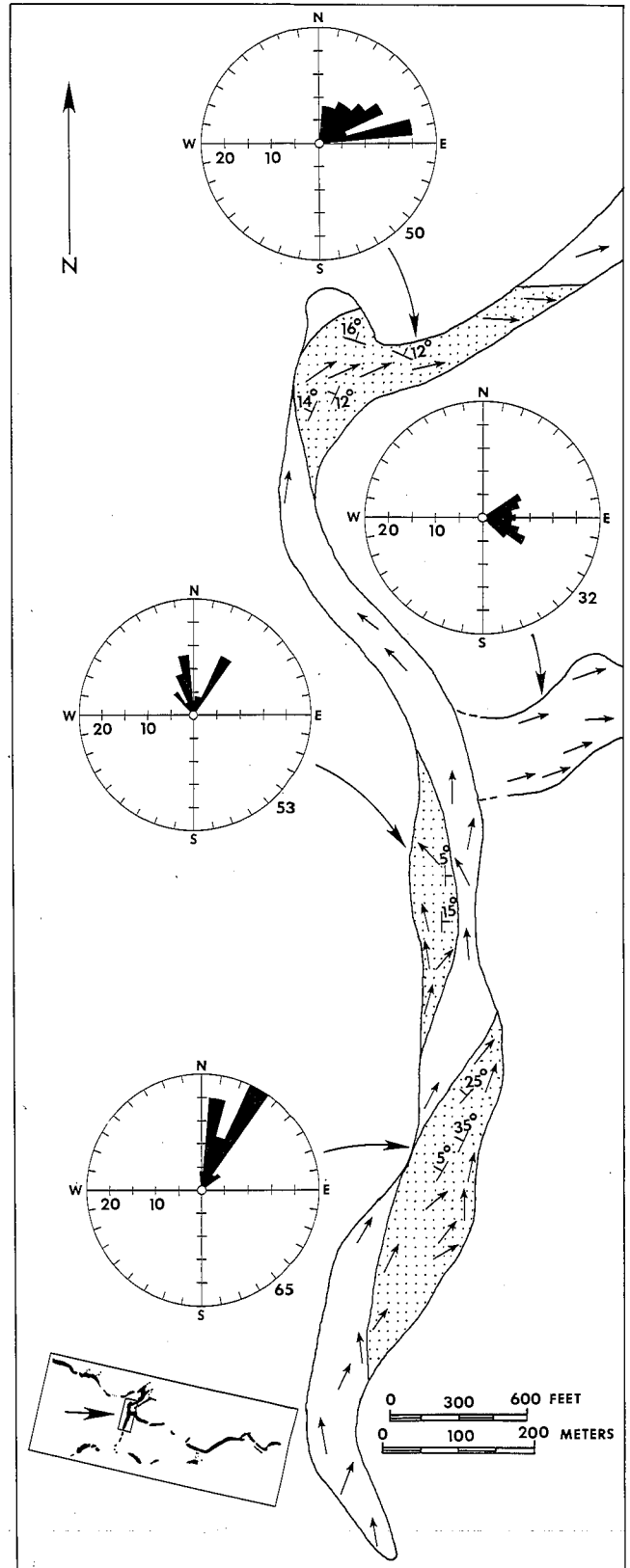


FIGURE 8.—Map of channel D, segment 6, and westernmost end of channel B.

they consist commonly of finer-grained sediment than that in the main channel course (fig. 11).

Channel Fills

The channel fills appear to have a more or less constant width along their lengths, except where recent erosion and undercutting have narrowed the channel remnants. The erosional contact at the base of the channels on the Cedar Mountain Shale appears to undulate. Pinching and swelling in channel thickness appear to correspond to pools and riffles found in modern stream channels. Thick channel-fill deposits are commonly found opposite point-bar deposits, and thin channel-fill deposits occur along straight reaches between channel bends. The channel-fill deposits generally erode to produce steep vertical walls (fig. 12). Parts of channels A and B have been significantly undercut to expose the concave bases of the channels. The preserved channel fills generally extend the complete length of each channel segment.

SEDIMENTARY STRUCTURES

Several sedimentary structures, both primary and diagenetic, are found on and within the paleochannels. Primary sedimentary structures have been studied because they indicate factors controlling sediment deposition, flow direction in paleochannels, and types of ancient environments. Diagenetic structures are secondary changes that occurred in the sediment after deposition.

Primary Structures

Primary sedimentary structures present in the four major paleochannels are trough cross-bedding, planar (tabular) cross-bedding, horizontal bedding, climbing ripples (ripple laminae), scour-and-fill deposits, and graded bedding. Trough cross-bedding (fig. 13) is the most common sedimentary structure present in the conglomeratic sandstone channels. According to Harms and Fahnestock (1965, p. 93) trough cross-beds have curved surfaces of erosion. Trough cross-bedding is considered to be one of the most reliable and precise paleocurrent indicators (High and Picard 1973, and Dott 1973) because of the

elongation of the trough axis and inclination of cross-strata.

Trough cross-beds are present in nearly all segments of the major paleochannels but appear to be extensive in channel B. Trough cross-beds are commonly recognizable in cross-sections along vertical sides of the paleochannels. Here current direction is difficult to measure because of the two-dimensional view of the cross-beds. Trough cross-bedding on several channel segments tends to dominate the sedimentary structures visible on the surface of the channels.

Planar cross-bedding (fig. 14) is present on all the major paleochannels but is particularly well exposed on the south side of channel A, at the western end of segment 2. At this point the channel bends to the south and then to the northeast. Along the southern part of the bend, planar cross-beds are observed on the surface of the channel and for approximately 2 m down the steep side of the channel fill. The planar bedding is commonly found dipping towards the center of the channel, perhaps because of weak lateral current flow on curved reaches of a channel, where cross-beds may have been deposited at low-flow stage where flow tended to conform to the concave channel bottom. Harms and Fahnestock (1965, p. 95) point out that planar cross-beds have bounded surfaces of cross-strata which are planar and parallel and are not bounded by trough-like erosional surfaces. The thickness of the planar cross-beds on the channels in the study area range from a few millimeters to 7 or 8 cm.

Ripple marks are rarely found on the paleochannels of the Cedar Mountain Formation. Stokes (1961, p. 168) also reports that ripple marks in sandstone channels of the Salt Wash Member of the Morrison Formation are relatively rare. Ripple marks are generally transverse to the current direction in relatively slow-moving water and are found throughout various depth ranges.

Climbing ripples (ripple lamination) form from the downstream migration of ripple marks under maximum sediment loads. They were observed along several segments of the major paleochannels. McKee (1965, p. 66) pointed out that ripple laminae are internal sediment structures, and ripple marks are generally surface forms. For example, climbing ripples (fig. 15)

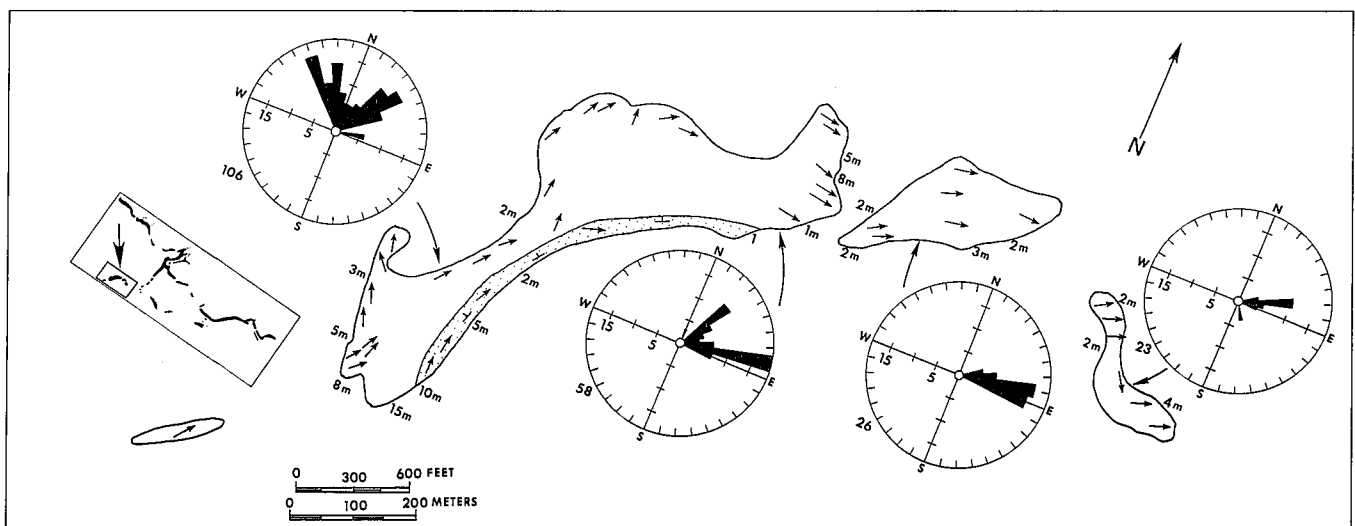


FIGURE 9.—Map of channel C, segments 2 and 3, showing current direction and thickness, in meters, along perimeter of segments.

are well exposed at several isolated locations along the west side of channel D, segment 6.

Scour-and-fill deposits are found throughout the channel sequence in every channel segment in the study area. Channel fills essentially grow from the process of scouring and deposition of sediment. All the channels in the study area exhibit lenses of pebble conglomerate filling scours in sandstone (fig. 16). These conglomerate lenses range from a few centimeters wide and deep to approximately 5–6 m wide and 4 m deep.

Examples of graded bedding can be found at nearly any locality on the major paleochannel. Beds show gradation in grain size from coarse below to fine above. Graded beds are present in nearly every sedimentary structure (fig. 17) discussed in this paper. Channels B, C, and D exhibit several major sequences of fining upward in the channels. Channel D, segment 6, shows as many as 6 major fining-upward sequences in the point-bar deposits. Channel A is different, however, because only one major coarsening-upward sequence occurs there. The channel fill is a single sequence from bottom to top.

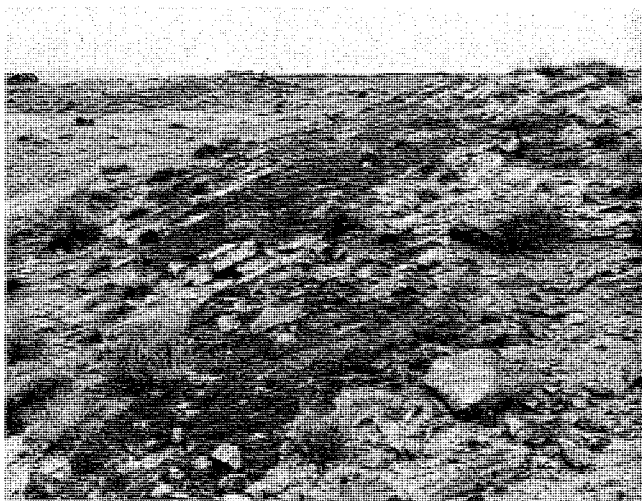


FIGURE 10.—Accretion ridge, which dips to the north, on a point-bar deposit in channel D, segment 6.

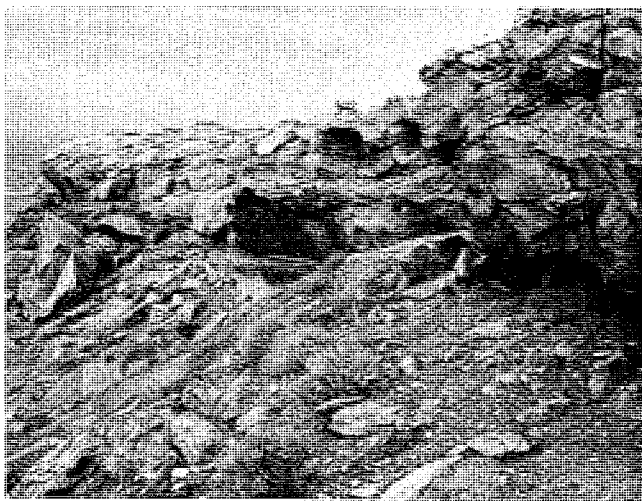


FIGURE 11.—Typical erosional surface of point-bar deposit. Ledges are approximately 2 m thick. Compare with figure 12.

Secondary Structures

Secondary structures occur in isolated areas throughout the major paleochannels. They occur within the channel fills and are principally iron-oxide concretions and silica crusts and structures.

Iron-oxide concretions are commonly present in sandstone but less commonly developed in the conglomerates. These concretions form spherical nodules that range in size from a few centimeters to approximately 0.7 m in diameter and are found as isolated spheric clusters along the surface of the channel fills. The nodules are limonite, with a distinctive yellow color. The limonite increases in density toward the center of each nodule.

Silica contributes to the formation of secondary structures common to all paleochannels in the thesis area. The silica bodies and the irregular silica crust have similar origins but form different structures. They form by chertification and silicification of grains and pebbles. Cementation appears to have an affinity for certain sedimentary structures and rock horizons. Most of the structures may have formed as a result of precipitation from fluids that could penetrate in areas of increased porosity and permeability in the channel, causing cementation

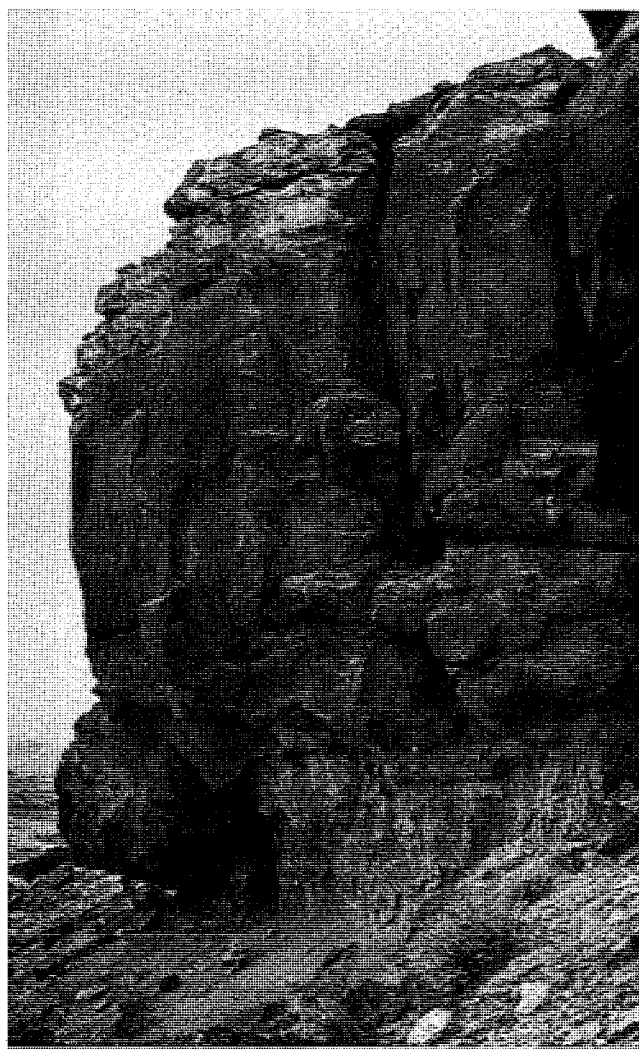


FIGURE 12.—Typical irregular basal erosion surface of channel-fill deposits. Approximate thickness of channel fill, channel C, segment 2, 15 m.

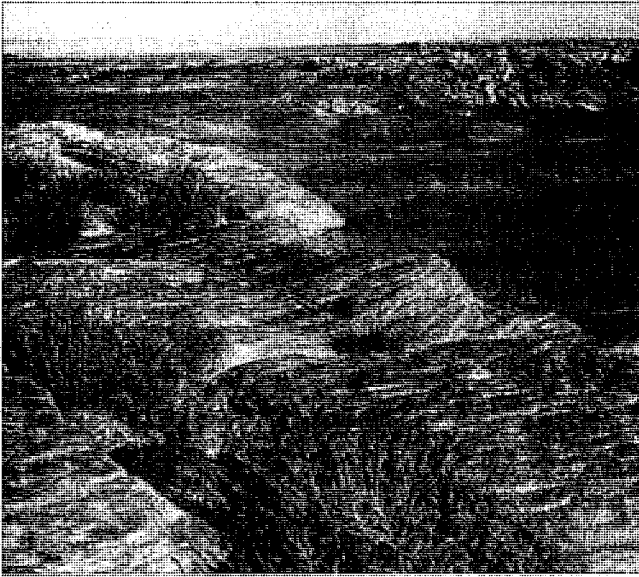


FIGURE 13.—Trough cross-beds typical of all channel segments of study area.

to cross sedimentary structures and rock boundaries. The major part of the paleochannels have calcite cementing, and in some areas on the paleochannels gradation can be recognized between calcite and chert. The silica cementation of grains and pebbles becomes hard and appears much like vitreous quartzite.

Silica bodies are lense shaped in cross section that appear to zigzag laterally through selected parts of the channel fill (fig. 18). These structures may be as large as 6 m wide and 1 m thick and extend up to 46 m long. The surface of nearly all the channel segments is littered with the remnants of chert-cemented sandstone from the silica structures. These siliceous bodies are found throughout the vertical sequence of the paleochannels, both in the point-bar deposits and the channel fills.

Silica crusts are similar to the silica bodies in composition but do not form any observable type of structure. They appear to cement several sets of cross-strata at one time and are gener-

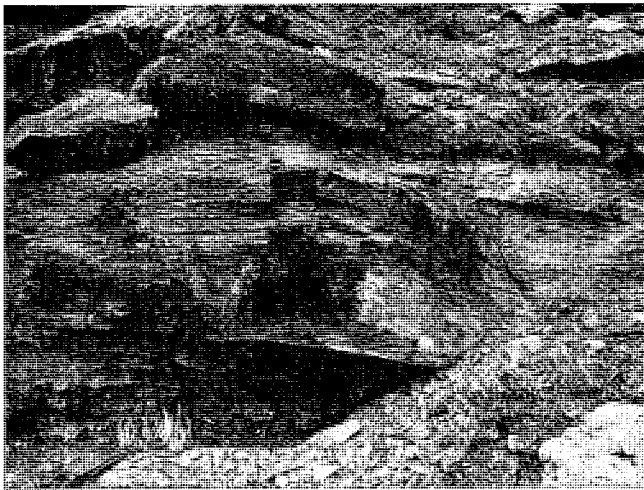


FIGURE 14.—Planar cross-beds gently dipping toward center of channel. Exposures near base of channel A, segment 2.

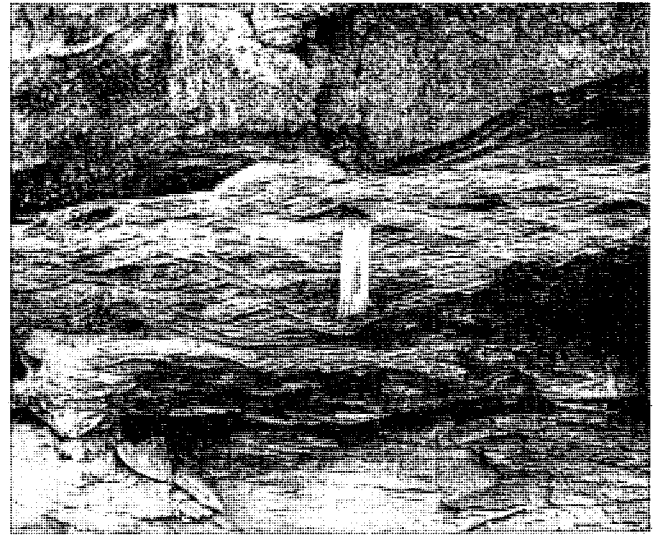


FIGURE 15.—Climbing ripples exposed in point-bar deposit in channel D, segment 6.

ally present at or near the surface of the channels. A silica crust nearly dominates the surface of channel D, segment 6.

The weathered surface of both chert-cemented bodies and crusts forms a polished dark brown varnish.

VERTICAL SEQUENCE

A characteristic vertical sedimentary sequence is readily definable in the paleochannels. Major differences occur in channel A, but channels B, C, and D are similar.

Channel A has one major sequence of fine upward (figs.

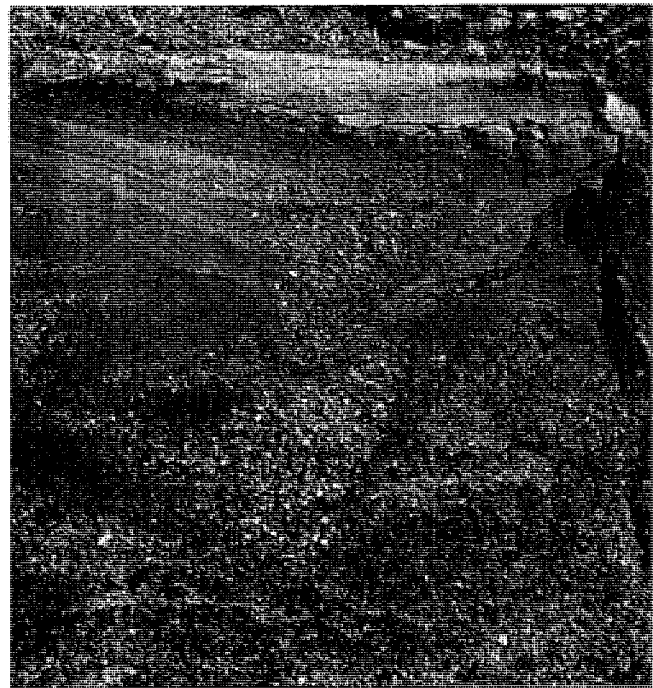


FIGURE 16.—Scour-and-fill deposits exposed in channel C, segment 2. Scours filled with chert pebbles. Base of photograph approximately 1.5 m.

19, 20). The lower fourth of the channel consists of coarse pebble conglomerate and clay nodules. This part of the channel is characterized by large-scale cross-beds ranging up to 0.9 m high. Small-scale cross-beds of coarse sediment occur between many of the large-scale cross-beds. A thick section near the base of the channel appears to be massive, unlayered pebble conglomerate. Pebbles of the conglomerate range in size from 2 to 3 cm in diameter but become finer until 2-mm-diameter material dominates. At this level the conglomerate abruptly grades to sand grains. Maximum pebble size ranges between 5 and 7 cm, and these pebbles are generally found as single fragments in the conglomerate.

The remainder of the sequence is predominately large-scale cross-bedded sandstone where some cross-beds are 1 m high. Planar cross-beds and climbing ripples commonly occur near the tops of the channel, but planar cross-beds have been observed through various sections of channel C from its surface to nearly the base of the channel. The surface of channel A is predominately light gray, well-sorted sandstone which shows large-scale trough cross-beds.

Channels B, C, and D are similar because they all have sev-

eral major fining-upward sequences. These sequences are only irregularly defined in the channel fills but are readily apparent in the point-bar deposits (fig. 21). The point-bar deposits rhythmically exhibit pebble- to sand-size material through both lateral and vertical sequences. In one fining-upward cycle the rocks exhibit both small- and large-scale cross-beds, with large-scale cross-beds dominating in the upper sandstone. Interbedding of single laminae of pebble conglomerate is common within the sandstones of both large and small cross-beds.

The basal parts of channels B, C, and D are similar to that of channel A in having a clay pebble zone.

PALEOCHANNEL CHARACTERISTICS

Factors of channel morphology influenced by the volume of water moving through a channel and the type of sediment load are width, depth, meander wavelength, gradient, shape, and sinuosity.

Data collected along modern alluvial rivers in Australia and the Great Plains of western United States have permitted Schumm (1972, p. 99-104) to develop empirical equations that

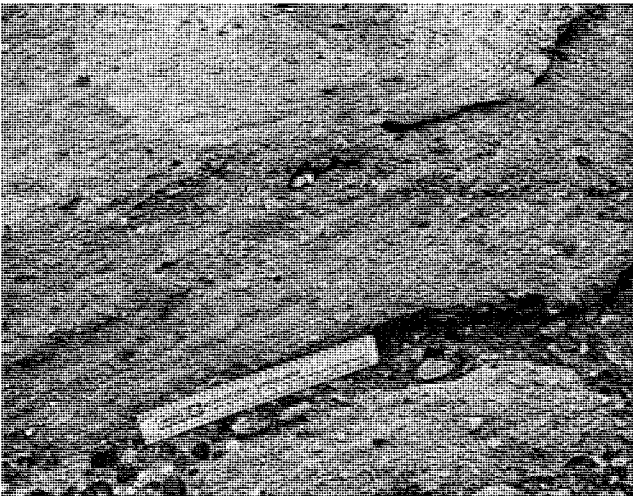


FIGURE 17.—Sequences of graded bedding exposures in trough cross-beds. Smaller trough cross-beds in upper center.

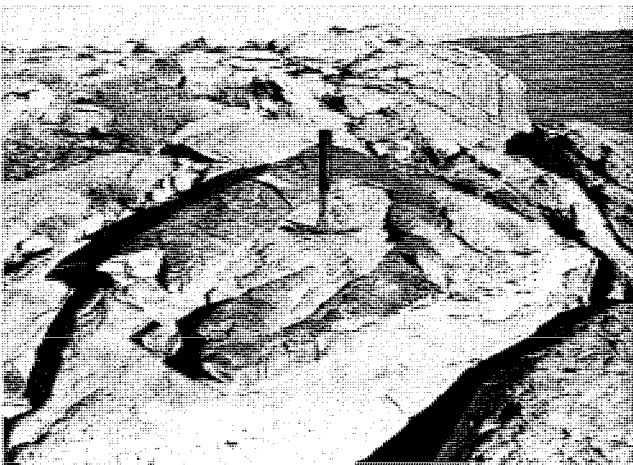


FIGURE 18.—Chert-cemented structure weathering from cross-bedded sandstone. Note three-dimensional feature of structure.



FIGURE 19.—Graded bedding near base of channel A, segment 2, exhibits lower, predominately clay nodule zone, grading up into chert pebble zone. Base of photograph approximately 1 m.

will estimate changes in the hydrologic regimen of a stream. These equations also permit the estimation of paleochannel gradient, meander wavelength, sinuosity, and discharge from channel dimensions.

Measurements of width, depth, and meander wavelength are easily obtained on the four major paleochannels from exposed cross sections in the channels.

Width and depth measurements of the Cedar Mountain channels were substituted in Schumm's (1972) equations, to provide approximate values on wavelength, gradient, and water discharge for each of the paleochannels in the area of study. Many of the values derived from Schumm's equations are generally not available in the rock record. Schumm (1972, p. 107) points out that the equations on paleochannel character provide only a reasonable estimate. Results of the calculations are recorded in table 1. These values indicate that channel width, depth, and meander wavelength will increase with increasing discharge, but channel gradient will decrease.

Current Direction

Maps were made of cross-bed orientation in deposits of four channels. Channel A, segment 2; channel B, segments 5, 6, 7, and 8; channel C, segments 1 and 2, and channel D, segment 6 with part of channel B, segment 1 (figs. 6, 7, 8, 9), were mapped. The cross-bed orientation patterns show current flow direction and help delineate point-bar and channel-fill deposits. The direction of sediment transport in each of the four major channels is in the direction of increasing segment numbers. Rose diagrams of current directions were plotted to show the variation in direction of sediment transport along relative short channel reaches. The dominant or average current and sediment transport direction for these four paleochannels are: Channel A—S 85° E, channel B—S 88° E, channel C—N 82° E, and channel D—N 8° E (fig. 2).

Channels A, B, and C all show subparallel eastward sediment transport. Channel D is the only one of the four major channels that flows in a northerly direction. Channel D is stratigraphically younger than the other three major paleochannels and may have started to flow northward because of local or regional tilting during deposition.

TABLE 1
Paleochannel Characteristics

Channel	F (w/d)	w (m)	d (m)	l (m)	s (m/k)	Q _{ma} (cms)	Q _m (cms)
A	5.3	32	6	480	0.28	215	20
B	10	75	7.5	1200	0.23	530	75
C	27.8	125	5	2935	0.37	600	80
D	10.8	70	7	1190	0.26	455	60

$$l = 18(F^{.53} w^{.69}),$$

$$s = 30 \frac{F^{.95}}{w^{.98}}$$

$$Q_{ma} = 16 \frac{w^{1.56}}{F^{.66}},$$

$$Q_m = \frac{w^{2.43}}{18F^{1.13}}$$

where l = meander wavelength in meters
 F = width to depth ratio of channel
 w = channel bank-full width in meters
 s = channel gradient in meters per kilometer
 Q_{ma} = flow during annual flood in cubic meters per second
 Q_m = mean annual discharge in cubic meters per second
 Schumm (1972)

Composition and Source Area

The four major paleochannels show similar modes of deposition and sediment composition of the conglomeratic sandstone. Field observation shows an abundance of chert pebbles in the conglomerates and quartz grains in the sandstone. This finding was supported by thin sections made from the four paleochannels. A centimeter grid was selectively placed over two areas on each thin section, and approximately 240 counts were made per thin section. Standard deviation and average percent of each grain type in channels A, B, C, and D are recorded in table 2.

Chert is the most abundant constituent of the pebble conglomerates. Eight to twelve percent of the pebble conglomerate contains fossil fragments in the chert pebbles. Fragments of the bryozoan *Stenopora*, fenestellid and twiggy cryptostome bryozoans, like the latter *Acanthocladia*, together with echinoderm and brachiopod fragments and monaxial sponge spicules of Permian age were observed in thin section.

A bleached, white bone was found in a cherty pebble conglomerate in channel C, segment 6, at the eastern end of the channel. The bone is approximately 18 cm long and appears to be the limb bone of a small Lower Cretaceous dinosaur (W. E. Miller pers. comm. 1979).

A common source area to the west or west-southwest for all four paleochannels is indicated by similarities in sediment composition, sedimentary structures, vertical sequence, and common Permian fossil fragments in the chert pebble conglomerates. A likely source area was the Sevier uplift that began in Upper Jurassic and continued through Cretaceous time (Hintze 1973, p. 75). The Sevier uplift trends north-northeast across the western part of Utah (Hunt 1956, p. 74). As the Se-

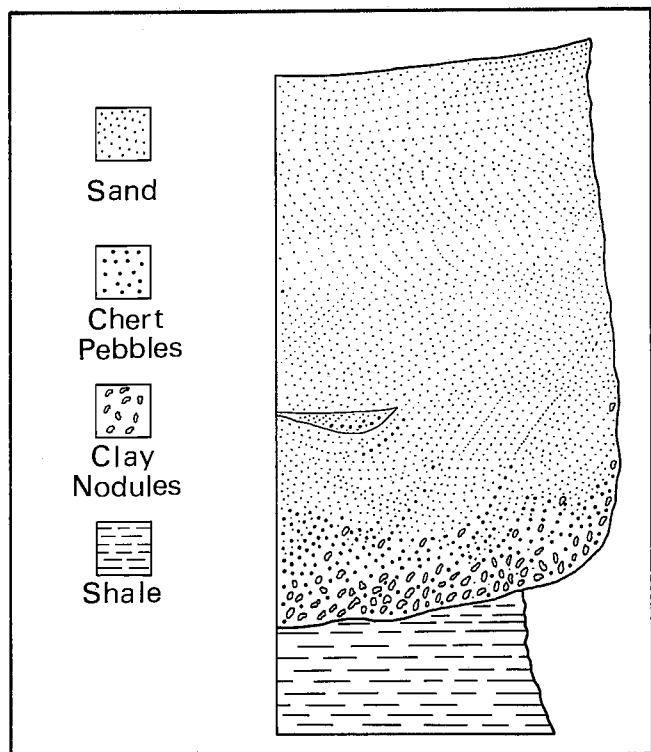


FIGURE 20.—Vertical sequence of channel A, showing major sequence of upward fining through channel fill.

vier uplift was rising, Permian beds were being eroded and transported to the east where they were deposited during Morrison and Cedar Mountain time (Hintze 1973, p. 63; Stokes 1972, p. 23).

CONCLUSIONS

The conglomeratic sandstone ridges in the Cedar Mountain Formation are of fluvial origin and have distinctive morphology and structure. The channel fills are divided into two major parts, point bars and channel-reach deposits which express different erosion patterns and internal structures. Point-bar deposits were built by lateral accretion. These layered rocks show accretion ridges on their upper surfaces. Laterally stratification dips into the paleochannels at from 1° to 40° .

The paleochannels exhibit low sinuosity, with sinuosity ratios between 1.2 and 1.5. This type of channel pattern is common in the middle to lower transporting segment of a river system.

The paleochannel characteristics were determined by formulae derived by Schumm (1968, 1972). The paleochannels had shallow gradients, ranging from 0.23 and 0.37 m/km. Annual discharge rate for the streams that produced the channels ranged from 215 to 600 m³/sec. Schumm (1972, p. 101) points out that channel width increases with discharge, which is associated with large meander wavelengths.

TABLE 2
Channel Composition

Channel	A		B		C		D	
	%	d*	%	d	%	d	%	d
chert	41	4.2	47	4.6	48	6.6	47	5.5
chert and fossils	9	3.2	11	4.2	8	1.5	12	10.5
siltstone	3	2.3	4	4.5	1	0.8	8	1.4
quartz	10	4.3	10	4.3	10	5.8	7	2.3
feldspar	1	0.8	—	—	—	—	—	—
carbonate	6	3.3	2	1.2	4	2.3	3	1.6
cement and matrix	30	2.7	26	2.8	29	6.5	29	7.0

* (d) is the standard deviation between six grain counts.

The channel fills of the Cedar Mountain Formation appear to be the last stage of fluvial deposition of sediments, transported eastward from the Sevier uplift before the study area was covered by shale deposited in the transgressive Cretaceous Mancos Sea.

REFERENCES CITED

- Allen, J. R. L., 1965, A review of the origin and characteristics of recent alluvial sediments: *Sedimentology*, v. 5, p. 89-191.
- Baker, A. A., Dane, C. H., and Reeside, J. B. Jr., 1936, Correlation of the Jurassic formations of parts of Utah, Arizona, New Mexico, and Colorado: U.S. Geological Survey Professional Paper 183, 66p.
- Brice, J. C., 1964, Channel patterns and terraces of the Loup Rivers in Nebraska: U.S. Geological Survey Professional Paper 422-D, 41p.
- Coffin, R. C., 1921, Radium, uranium, and vanadium deposits of southwestern Colorado: Colorado Geological Survey Bulletin 16, 231p.
- Coleman, J. M., 1969, Brahmaputra River: Channel processes and sedimentation: *Sedimentary Geology*, v. 3, p. 129-239.
- Derr, M. E., 1974, Sedimentary structures and depositional environment of paleochannels in the Jurassic Morrison Formation near Green River, Utah: Brigham Young University Geology Studies, v. 21, pt. 3, p. 3-39.
- Dott, R. H., Jr., 1973, Paleocurrent analysis of trough cross-stratification: *Journal of Sedimentary Petrology*, v. 43, p. 779-83.
- Fisk, H. N., 1947, Fine-grained alluvial deposits and their effects on Mississippi River activity: Mississippi River Commission, Vicksburg, Mississippi, 82p.
- Harms, J. C., and Fahnestock, R. K., 1965, Stratification, bed forms, and flow phenomena (with an example for the Rio Grande): In Middleton, G. V. (ed.), Primary sedimentary structures and their hydrodynamic interpretation: Society of Economic Paleontologists and Mineralogists Special Publication 12, p. 84-115.
- High, L. R., and Picard, M. D., 1973, Reliability of cross-stratification types as paleocurrent indicators in fluvial rocks: *Journal of Sedimentary Petrology*, v. 44, p. 158-68.
- Hintze, L. F., 1973, Geologic history of Utah: Brigham Young University Geology Studies, v. 20, pt. 3, 181p.
- Hunt, C. B., 1956, Cenozoic geology of the Colorado Plateau: U.S. Geological Survey Professional Paper 279, 99p.
- Katich, P. J., 1951, Recent evidence for Lower Cretaceous deposits in Colorado Plateau: American Association of Petroleum Geologists Bulletin, v. 35, no. 9, p. 2093-94.
- Lane, E. W., 1957, A study of the shape of channels formed by natural streams flowing in erodable material: U.S. Army Corps of Engineers (Omaha), Missouri River Division Sediment Series, no. 9, 106p.
- Lawyer, G. F., 1972, Sedimentary features and paleoenvironment of the Dakota Sandstone (early Upper Cretaceous) near Hanksville, Utah: Brigham Young University Geology Studies, v. 19, pt. 2, p. 89-120.

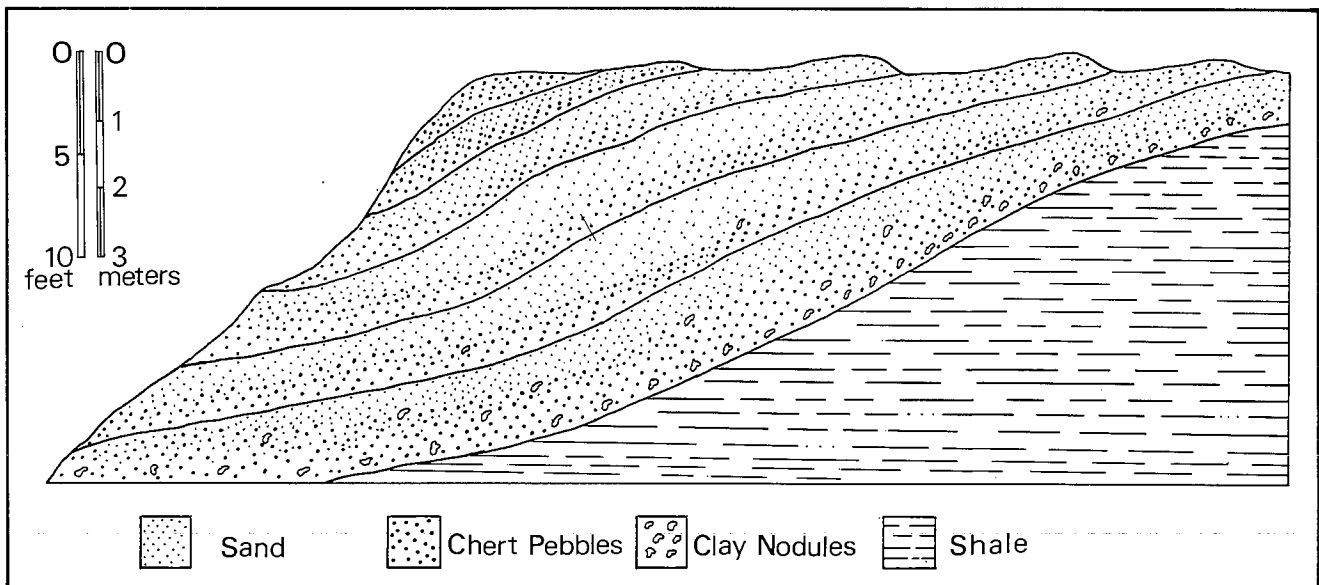


FIGURE 21.—Cross-section of point-bar deposit exhibiting several sequences of upward fining.

- Leopold, L. B., and Wolman, M. G., 1957, River channel patterns: braided, meandering, and straight: U.S. Geological Survey Professional Paper 282-B, 51p.
- _____, 1960, River meanders: Geological Society of America Bulletin, v. 71, p. 769-94.
- McKee, E. D., 1965, Experiments on ripple lamination: In Middleton, G. V. (ed.), Primary sedimentary structures and their hydrodynamic interpretation: Society of Economic Paleontologists and Mineralogists Special Publication 12, p. 84-115.
- Mook, C. C., 1916, A study of the Morrison Formation: New York Academy of Sciences Annals, v. 27, p. 39-191.
- Moody-Stuart, M., 1966, High- and low-sinuosity stream deposits, with examples from the Devonian of Spitsbergen: Journal of Sedimentary Petrology, v. 36, p. 1102-17.
- Russell, R. J., 1954, Alluvial morphology of Anatolian rivers: Association of American Geographers Annals, v. 44, p. 363-91.
- Schumm, S. A., 1963, Sinuosity of alluvial rivers on the Great Plains: Geological Society of America Bulletin, v. 74, p. 1089-1100.
- _____, 1972, Fluvial paleochannels: In Rigby, J. K., and Hamblin, W. K. (eds.), Recognition of ancient sedimentary environments: Society of Economic Paleontologists and Mineralogists Special Publication 16, p. 98-107.
- _____, 1977, The fluvial system: John Wiley and Sons, New York, 338p.
- Shelton, J. W., and Noble, R. L., 1974, Depositional features of braided-meandering streams: American Association of Petroleum Geologists Bulletin, v. 58, p. 742-52.
- Stokes, W. L., 1944, Morrison Formation and related deposits in and adjacent to the Colorado Plateau: Geological Society of America Bulletin, v. 55, p. 951-92.
- _____, 1952, Lower Cretaceous in Colorado Plateau: American Association of Petroleum Geologists Bulletin, v. 36, p. 1766-76.
- _____, 1961, Fluvial and eolian sandstone bodies in the Colorado Plateau: In Petersen, J. A., and Osmond, J. C. (eds.), Geometry of sandstone bodies—A symposium: American Association of Petroleum Geologists, 45th Annual Meeting, p. 151-78.
- _____, 1972, Stratigraphic problems of the Triassic and Jurassic sedimentary rocks of central Utah: Utah Geological Association Publication 2, p. 21-28.
- Stokes, W. L., Phoenix, D. A., 1948, Geology of the Egnar-Gypsum Valley area, San Miguel and Montrose Counties, Colorado: U.S. Geological Survey Preliminary Map 93, Oil and Gas Investigation Service.
- Trimble, L. M., and Doelling, H. H., 1978, Geology and uranium-vanadium deposits of the San Rafael River mining area, Emery County, Utah: Utah Geological and Mineralogical Survey Bulletin 113, 112p.
- Young, G. R., 1960, Dakota Group of Colorado Plateau: American Association of Petroleum Geologists Bulletin, v. 44, p. 156-94.